

ASPECT Hackathon 2018 Final report

ASPECT Hackathon 2018 Final report	1
Introduction	4
Timeline	5
Participants and areas of interest	6
Report on projects the participants worked on	9
Status Badges on the main ASPECT github page	9
Timo Heister, Lorraine Hwang	9
Unit tests	9
Timo Heister	9
C++11 standard	9
Timo Heister	9
2.0.1 release	10
Rene Gassmoeller, Timo Heister	10
Add Calculation of RMS Velocity Over the Area of Each Boundary	10
Paul Bremner	10
Allow compositional fields to be advected with the melt velocity	10
Juliane Dannberg	10
Implementing heat flux boundary conditions	10
Juliane Dannberg, Jonathan Kay, Rene Gassmoeller	10
Implementation of a depth dependent shear wave to density scaling	11
Jacky Austermann	11
Set Dirichlet boundary conditions only for inflow boundaries	11
Juliane Dannberg, Timo Heister	11
Implement an interface for flexible surface deformation	12
Rene Gassmoeller	12
PerpleX live material model	12
Bob Myhill	12
Modified Tait material model	12
Bob Myhill	12
Multicomponent compressible material model	13
Bob Myhill	13
Document addition: Thermodynamic self-consistency	13
Bob Myhill	13
Viscoplastic thermal convection benchmark (Tosi et al. 2015)	13
Anne Glerum	13
Prescribed boundary velocities using spherical unit vectors	14

Bart Niday	14
Tests for strain localization with strain weakening	15
Arushi Saxena	15
Implementing a high resolution upper mantle tomography grid (on top on S40RTS)	16
Sophie Coulson	16
A cookbook for the adiabatic boundary as initial temperature condition	17
Emmanuel Njinju	17
Visualization of the strain rate tensor	18
Bart Niday	18
Implementation of the NSinker benchmark	19
Rene Gassmoeller, Cedric Thieulot, Conrad Clevenger, Timo Heister	19
Implementation of adjoint sensitivity kernels	20
Jacky Austermann	20
Calculation of gravity anomalies in geoid postprocessor	21
Jacky Austermann and Ludovic Jeanniot	21
Implementation of a depth-dependent initial temperature plugin	21
Marie Kajan	21
Set up a 3D subduction model for South America	22
Diandian Peng	22
Parse map utility function	22
Paul Bremner	22
Implementing a viscoelastic-plastic rheology	23
John Naliboff	23
2D analytical benchmark, part 1	24
C. Thieulot	24
2D analytical benchmark, part 2	25
C. Thieulot	25
Implementation of stabilised Q1Q1 element	26
C. Thieulot & W. Bangerth	26
Implement new properties in the visualization for melt material properties	26
Joe Schools	26
New postprocessor plugin to calculate the seismic velocities and velocity anomalies in models with melt	27
Joe Schools	27
New postprocessor to compute gravity acceleration and potential	28
Ludovic Jeanniot, John Naliboff, and Cedric Thieulot	28
Speed up the assembly for the Newton solver	30
Menno Fraters and Rene Gassmoeller	30
Added test for the isotherms pull request	32
Menno Fraters	32
World builder structure	33
Menno Fraters	33

Tracking the plastic and/or viscous strain	34
Anne Glerum	34
Postprocessor to calculate the grain orientation lag parameter	35
Hannah Mark	35
Option to skip solvers and initial conditions during pre-refinement	36
Ludovic Jeanniot and Wanying Wang	36
3D thermal convection benchmark in a spherical shell by Arrial et al. 2014	37
Ludovic Jeanniot and Cedric Thieulot	37
A cookbook for convection on icy satellites	38
Jonathan Kay	38
Testing new ‘GMRES solver restart length’ parameter	39
Marie Kajan	39
Development of a benchmark for active tracer particles in ASPECT	40
Gerry Puckett	40
Regionally high resolution 3D spherical flow model with weak plate boundaries	41
Wanying Wang	41
Implement lateral viscosity variations for multiple structures	42
Wanying Wang	42
Statistics about ASPECT’s growth during the hackathon	43
References	43

Introduction

To further develop the mantle convection code ASPECT and to grow and foster its user community, 24 users and developers of ASPECT worked side-by-side over a 9 day period close to Petaluma, California in June 2018.

During this time the ASPECT community made substantial progress in various areas of development of the code as well as improving its workflow and generating new ideas for future development.

An area of particular interest among participants was the modeling of plastic and other non-standard rheologic behavior and its effect in realistic applications. Accordingly, improvements were made in tracking viscous/plastic strain, applications of rheologies for convection in icy satellites, tracking finite strain and grain-size parameters, testing the influence of visco-elasto-plasticity and strain weakening, improving the robustness of models with plastic yielding and the setup of models with compositionally dependent viscosity.

A second area of interest was the comparison of model results to observations, and the use of observations as initial conditions for models. Improvements include depth-dependent velocity-to-density scalings for tomography models, merging regional and global seismic models into a single initial condition, and computing seismic velocities in models with two-phase flow. Additionally, new postprocessors for the computation of gravity anomalies were added, and progress was made on solving adjoint equations to compute the sensitivity of model results to uncertainties.

A third focus of the hackathon included a benchmarking effort and improved thermodynamic consistency of the employed material properties. Several new benchmarks for 2D and 3D flow, both with analytical solutions and comparisons to other published and unpublished software were created and added to the set of existing benchmarks. Beyond that, progress was made in making material descriptions more consistent thermodynamically. This includes new guidelines for how to relate material properties to each other in a way that is thermodynamically consistent, and several new, fully thermodynamically consistent material models, one of which couples to the PerpleX software, and others that implement previously published equations of state.

Finally, a number of numerical and software design improvements were made to improve convergence behavior and runtime for hard model problems, leading to speedups in assembly time of a factor of two (for the Newton solver), speedup in solver time of a factor of up to 4 (for instantaneous models with expensive initial conditions and refinement), or to allow convergence at all that was not possible before (for moderately refined 3D spherical models with viscosity contrasts of up to 7 orders of magnitude).

During the course of the hackathon, every participant contributed source code to the project.

Together, users and principal developers added a total of more than 4,000 lines of code, arising from 176 individual contributions, and including 40 new tests. These numbers are slightly lower than for the last hackathon, in line with the slightly reduced duration (9 instead of 10 days).

Below is the timeline and a description of the individual contributions.

Timeline

Day	Scheduled items
Monday, 06/18	Arrival 5pm: All maintainers exchange ideas, plan workflow 8pm: House rules, Organization (Lorraine), Introductions
Tuesday, 06/19	9am: Individual topic introductions, create teams 9:30am: Git Pull Requests (Timo, Wolfgang) 10:30am PyLith: What are finite elements? (Matt) 11:30am PyLith: Overview of code layout (Brad)
Wednesday, 06/20	9am: Combined morning rounds (Rene) 9:30am: Public pull request review (Rene) 9:30am PyLith: Implementation steps 1:00pm PyLith: Method of Manufactured Solutions for testing
Thursday, 06/21	9am: Separate morning rounds 1:30pm: Adjoint equations (Jacky)
Friday, 06/22	9am: Combined morning rounds 1:30pm: ASPECT release procedure (Timo) Evening: Campfire
Saturday, 06/23	9am: Morning rounds Pylith Pylith wrap-up day ASPECT Day off Dinner on your own
Sunday, 06/24	Pylith departure day 9am: Morning rounds 1pm: Introduction to IDEs (Eclipse, QtCreator)
Monday, 06/25	1pm: Geometric multigrid preconditioner (Timo)
Tuesday, 06/26	9:30am: Newton solver (Menno) 1pm: Presentation of unit test framework (Timo) Dinner: Group dinner in Petaluma or at the beach

Wednesday, 06/27	Finish projects
Thursday, 06/28	Check-out and departure 10am

Participants and areas of interest

Name, affiliation, email	Goals and interests for this hackathon
Rene Gassmoeller, UC Davis, rene.gassmoeller@mailbox.org	<ol style="list-style-type: none"> 1. Help others achieve their goals 2. Review pull requests 3. Improve tester setups 4. Cleanup duty
Lorraine Hwang UC Davis lhwang@ucdavis.edu	<ol style="list-style-type: none"> 1. Logistics 2. Reproducibility and JupyterLab 3. Logistics 4. Discussions on data and publishing 5. Logistics 6. Reporting
Wolfgang Bangerth Colorado State University bangerth@colostate.edu	<ol style="list-style-type: none"> 1. Review pull requests 2. Help others 3. Write documentation 4. Deal with the reference viscosity mess 5. Benchmark why Newton assembly is so slow (with Menno and Rene)
Juliane Dannberg UC Davis judannberg@gmail.com	<ol style="list-style-type: none"> 1. Help others 2. Review pull requests 3. Make operator splitting faster 4. If there is time, extend melt transport models
Timo Heister Clemson University heister@clemson.edu	<ol style="list-style-type: none"> 1. Review pull requests 2. Help others 3. Infrastructure work (testing, cmake, etc.) 4. Linear solvers (multigrid, Schur complement) 5. Geometry representation
Jacky Austermann Columbia University ja3170@columbia.edu	<ol style="list-style-type: none"> 1. Adjoint equations (esp. gravity in objective functional and implementing iterative material model update / inversion) 2. Self-gravity (for surface observables and / or within model domain) 3. Viscoelastic benchmarks
Menno Fraters Utrecht University menno.fraters@outlook.com	<ol style="list-style-type: none"> 1. Add Newton benchmarks to repository 2. Merge core structure of world generator plugin 3. Review pull requests

	4. Help others
Jonathan Kay Lunar and Planetary Institute kay@lpi.usra.edu	1. Learn basics of GIT and ASPECT 2. Implement icy convection model 3. Add temperature dependent conductivity
Hannah Mark MIT/WHOI hmark@whoi.edu	1. Learn basics of ASPECT and C++ 2. Extend finite strain cookbook to calculate grain orientation lag 3. Try using strain history to update viscosity?
Sophie Coulson Harvard University slcoulson@g.harvard.edu	1. Learn basics of ASPECT and C++ 2. Read in gridded Vs data and convert to temperatures 3. Create initial temperature condition using high resolution regional seismic tomography model as a patch in lower resolution global model
Paul Bremner University of Florida pbremner@ufl.edu	1. Starter projects 2. Clear up declaring field values in various material model plugins 3. Help to link PerpleX/Burnman output and ASPECT. 4. Help with Vp/Vs postprocessor output
Bob Myhill University of Bristol bob.myhill@bristol.ac.uk	1. Starter projects (fix gnuplot output, max iterations) 2. Link PerpleX and ASPECT 3. Add cookbook illustrating effects of governing equation approximations ... not happening
Arushi Saxena University of Memphis asaxena@memphis.edu	1. Implement non local plasticity. 2. Work on lithospheric foundering. 3. Work on starter projects.
Emmanuel Njinju Virginia Tech njinju85@vt.edu	1. Work on completing the cookbook for the adiabatic boundary. 2. Work on a density model with reference density at the adiabatic boundary
Wanying Wang University of Texas at Austin wanying@utexas.edu	1. Learn Git with starter project 2. Speed up and improve model resolution for models with viscosity and density structures
Bart Niday University of Oregon wniday@uoregon.edu	1. Extend integrated strain tracers to calculate proxies for anisotropy 2. Do starter projects 3. Think about material model with 'function' for equations

Diandian Peng University of Illinois at Urbana-Champaign	<ol style="list-style-type: none"> 1. Learn ASPECT and Git 2. Do starter projects 3. Setup subduction models with ASPECT
Ludovic Jeanniot Utrecht University l.jeanniot@uu.nl	<ol style="list-style-type: none"> 1. Finish gravity post-processor, add a test and write a cookbook 2. check the crust 1.0 material model and use the post-processor on chunk geometry with crust 1.0 3. Thermal convection benchmark
Anne Glerum GFZ Potsdam acglerum@gfz-potsdam.de	<ol style="list-style-type: none"> 1. Setup framework for interaction with surface processes codes 2. Help with viscoelastoplastic material model 3. Add benchmarks 4. Subduction cookbook
Joe Schools University of Maryland jschools@umd.edu	<ol style="list-style-type: none"> 1. Implement simple thermodynamic integrations 2. Improving melt migration post processors, visualizations 3. Improving Vp/Vs post processor, get it working with more material models
Marie Kajan University of Florida marie.kajan@gmail.com	<ol style="list-style-type: none"> 1. Write test(s) to finalize 'ascii profile' initial temperature plugin 2. Test/improve adaptive mesh refinement in 3-D spherical geometry 3. Identify/solve issues involving simulations with complex 3-D structure and material parameters
Cedric Thieulot Utrecht University c.thieulot@uu.nl	<ol style="list-style-type: none"> 1. Designed new analytical benchmark with viscosity contrast control 2. Implement Q1Q1-stab element 3. Annulus convection cookbook
Elbridge Gerry Puckett U.C. Davis egpuckett@ucdavis.edu	<ol style="list-style-type: none"> 1. Learn from participants if they are interested in using particles for their work and, if so, how. 2. Work on new idea for particle capability(s) 3. Work on convergence rate estimator based on Richardson Extrapolation for problems when no exact solution is known
John Naliboff U.C. Davis jbnaliboff@ucdavis.edu	<ol style="list-style-type: none"> 1. Implement a VEP material model 2. Help others with projects 3. Add new material model tests 4. Review pull requests

Report on projects the participants worked on

Status Badges on the main ASPECT github page

Timo Heister, Lorraine Hwang

To better follow best practices of Software publication ASPECT's github homepage (<https://github.com/geodynamics/aspect>) now includes badges that mention its license, a Zenodo reference to the latest release, and a build status of the latest test results.

The following screenshot shows the current set of badges:

ASPECT - Advanced Solver for Problems in Earth's Convection

license [GPL](#) DOI [10.5281/zenodo.1296540](#) build [running](#)

About

Unit tests

Timo Heister

We now have a framework for unit tests in place (with several examples already in the code). The tests are in `unit_tests/*cc` and can be run using “make test”, “make run_unit_tests”, “ctest”, or using “`./aspect --test`”:

```
heister@timot470p /ssd/aspect-git/build (unit_test-vector-example) $ 
heister@timot470p /ssd/aspect-git/build (unit_test-vector-example) $ ./aspect --test
=====
All tests passed (20 assertions in 4 test cases)
```

C++11 standard

Timo Heister

We now require the c++11 standard, which allows us to use various new C++ features including lambda functions, range-based for loops, move constructors, initializer lists, auto, etc.. Various pull requests to modernize the code are in progress or already merged.

2.0.1 release

Rene Gassmoeller, Timo Heister

We finished and released the 2.0.1 bug fix release. The changes are documented here:

<https://geodynamics.org/cig/software/aspect/>

Add Calculation of RMS Velocity Over the Area of Each Boundary

Paul Bremner

The “velocity boundary statistics” postprocessor previously only calculated the minimum and maximum velocities over each boundary. Now it also computes the root mean square velocity over these same boundaries. These velocities are written both to the screen output and new columns in the statistics output file and are useful to compute quantities like the surface mobility (boundary rms-velocity over volumetric rms-velocity), which is a measure for plate-tectonic like behavior.

Allow compositional fields to be advected with the melt velocity

Juliane Dannberg

Compositional fields that represent properties that are primarily transported by melt can now use the melt velocity instead of the solid material to be transported. This was achieved by adding a new ‘type’ of compositional field called ‘melt field’.

Implementing heat flux boundary conditions

Juliane Dannberg, Jonathan Kay, Rene Gassmoeller

Previously we only had Dirichlet boundary conditions for the temperature, or Neumann boundary conditions that prescribe a zero heat flux. We added a new plugin type and an assembler that allows to prescribe non-zero heat flux boundary conditions in a weak sense. This is useful for example for models of satellites with basal tidal heating, or crustal-scale models with a prescribed heat-flow from the lithosphere.

Implementation of a depth dependent shear wave to density scaling

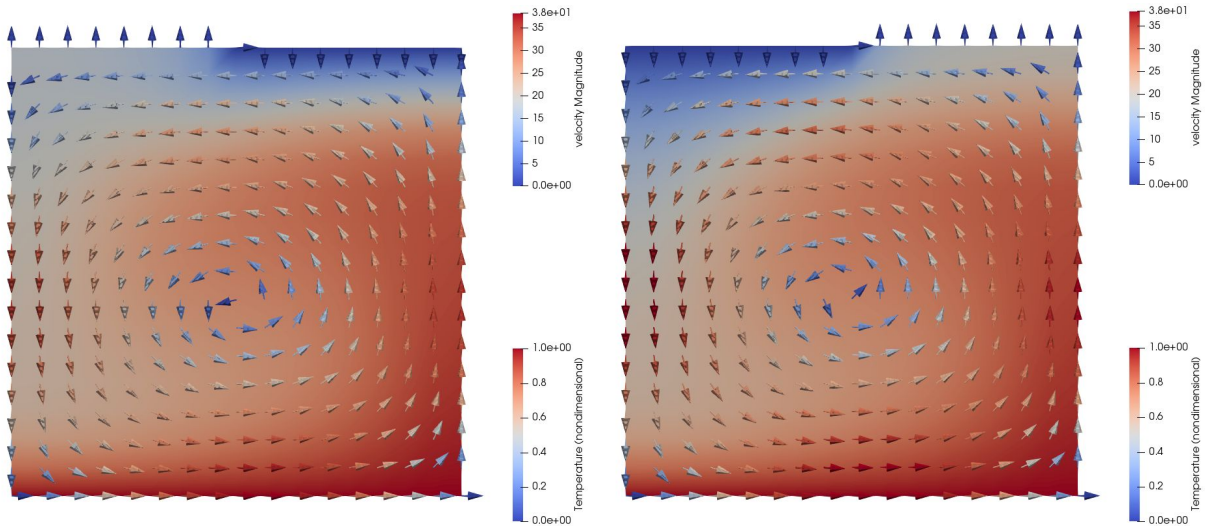
Jacky Austermann

When using a shear wave tomography model (e.g. S40RTS, SAVANI) as input for an initial temperature field one has to specify how shear wave velocity should be converted into density. Up to now this conversion factor was a constant that is specified by the user. I have now implemented the possibility to choose between either keeping this factor a constant or reading in a depth-varying factor from an ascii file.

Set Dirichlet boundary conditions only for inflow boundaries

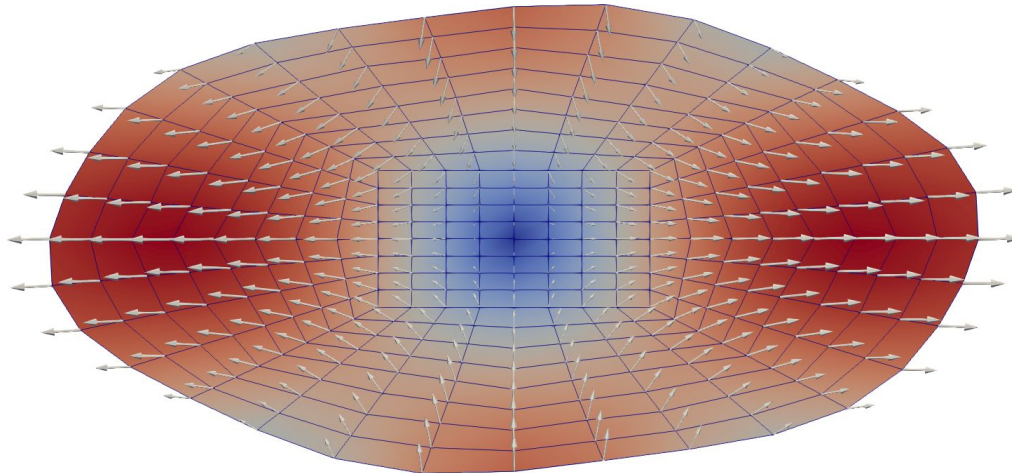
Juliane Dannberg, Timo Heister

Dirichlet boundary conditions for advected fields used to be prescribed on the whole boundary, independent of the flow field. However, physically, Dirichlet boundary conditions only make sense on an inflow boundary, or boundaries with parallel flow. We added an option that allows a user to prescribe the temperature and/or composition only on inflow, but not on outflow boundaries. The figure below shows a simple convection box model with time-dependent in- and outflow at the top boundary that illustrates this change. Note how the temperature at the surface (background temperature) changes in dependence of the flow field (arrows).



Implement an interface for flexible surface deformation

Rene Gassmoeller



I updated our draft for an interface that allows arbitrary surface deformation. This interface can be used for modeling a combination of a free surface and a prescribed deformation mechanism like crystallization of additional material, or rotational forces (for fast spinning bodies). It will also be used as a starting point for including surface evolution processes into ASPECT (either as simplified implementation into ASPECT itself, or as an interface to another software).

PerpleX live material model

Bob Myhill

ASPECT can now call PerpleX on-the-fly during a model run to compute the material coefficients. The contrib/perplex folder contains a setup script to download PerpleX and create a shared library that can be read and used by ASPECT. This allows much more thermodynamically consistent models than the previously available precomputed lookup-table approach. However, it is also significantly slower.

Modified Tait material model

Bob Myhill

ASPECT now includes a fully self-consistent compressible material model that implements the equation of state contained within Holland and Powell (2011).

Multicomponent compressible material model

Bob Myhill

ASPECT now includes a fully self-consistent simple compressible material model that implements the Murnaghan equation of state coupled with a simplified thermal-pressure term. This model can run a composite model built from multiple materials with different equation of state coefficients.

Document addition: Thermodynamic self-consistency

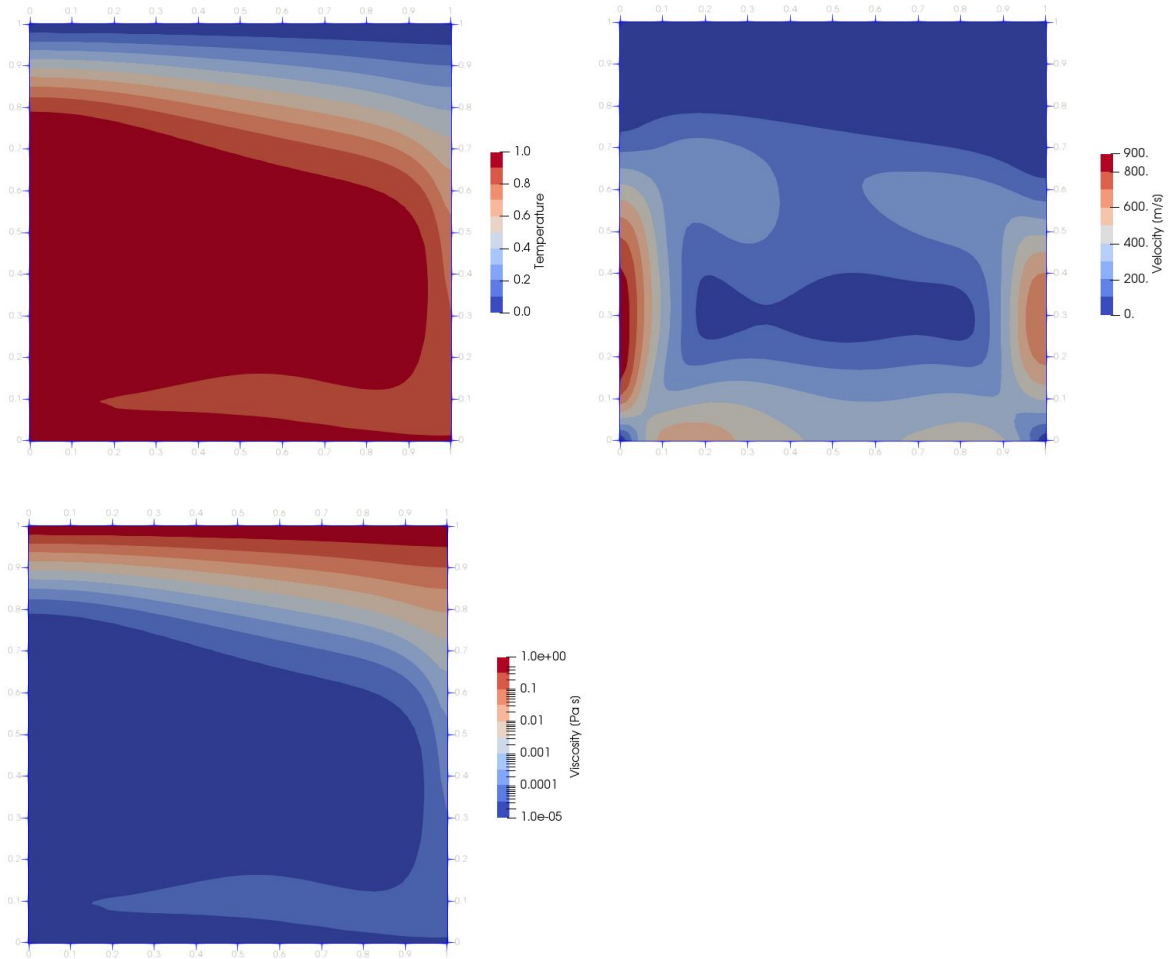
Bob Myhill

Material models in ASPECT can define material properties completely independently, but there are thermodynamic relations that should be obeyed for self-consistency. The manual now contains details of the requirements for a self-consistent material model (Section 2.2.1).

Viscoplastic thermal convection benchmark (Tosi et al. 2015)

Anne Glerum

I have included the 5 benchmark cases of the paper by Tosi et al. (2015) that compared results for 11 different codes, including ASPECT. The benchmarks consider viscoplastic thermal convection in a box, with different combinations of temperature-, depth- and strain rate dependent viscosity contributions. The figure below shows the steady-state results for Case 1, which can be compared to Fig. 1 of the original paper.

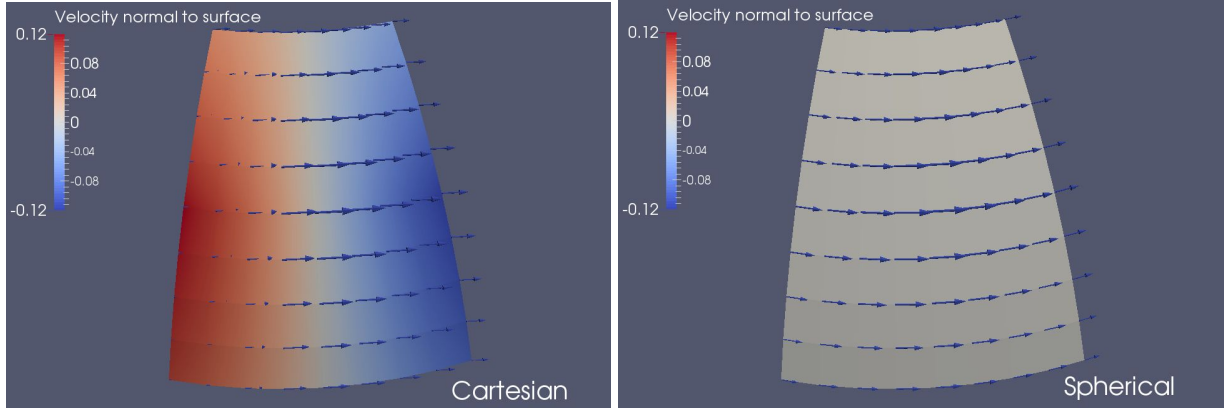


Case 1: steady-state solutions of the temperature and velocity and the resulting temperature-dependent viscosity field.

Prescribed boundary velocities using spherical unit vectors

Bart Niday

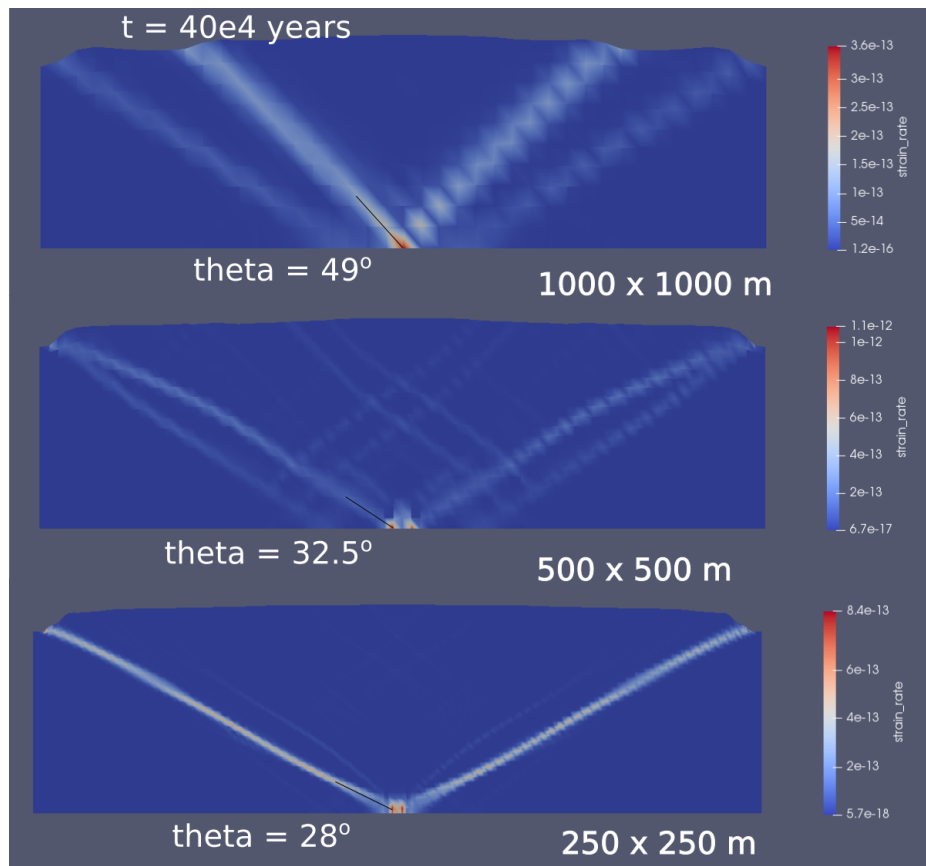
Boundary velocity plugins used to require input in Cartesian coordinates, regardless of the geometry model. This meant that in spherical models, ascii boundary condition files had to be converted to the internal ASPECT coordinate system. Now there is an option for the plugins to work in spherical coordinates (i.e. vertical, north, and east components of the velocity). This option also interpolates ascii boundary conditions in spherical rather than Cartesian coordinates, which might be better for e.g. tangential plate motions on the surface, or at least makes it substantially easier to input data. The figures show the difference between interpolation in spherical and Cartesian coordinates.



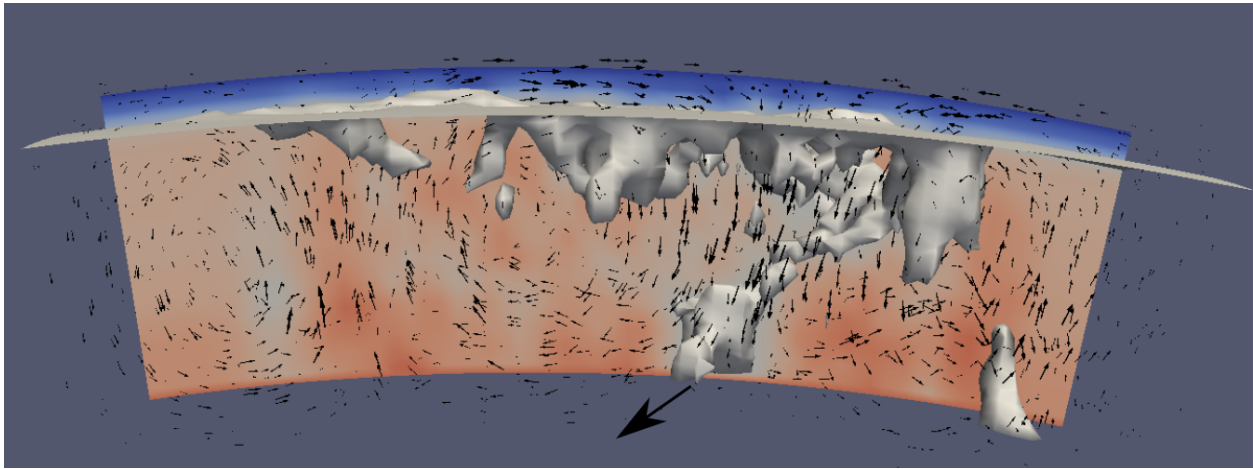
Tests for strain localization with strain weakening

Arushi Saxena

We tested the behavior of strain localization for material models with strain weakening, and reproduced the results of Kaus, 2010. The model below shows that the shear angles converge towards the Coulomb angle (theta = 30 degrees) during increasing compression:



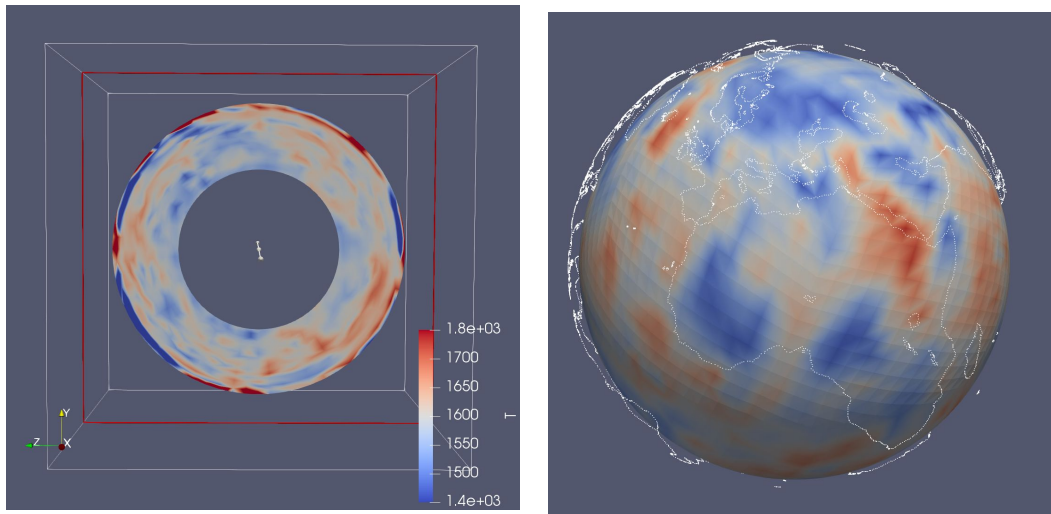
The model is based on the lithospheric foundering model proposed from the seismic tomography results of Biryol et al., 2016:



Implementing a high resolution upper mantle tomography grid (on top on S40RTS)

Sophie Coulson

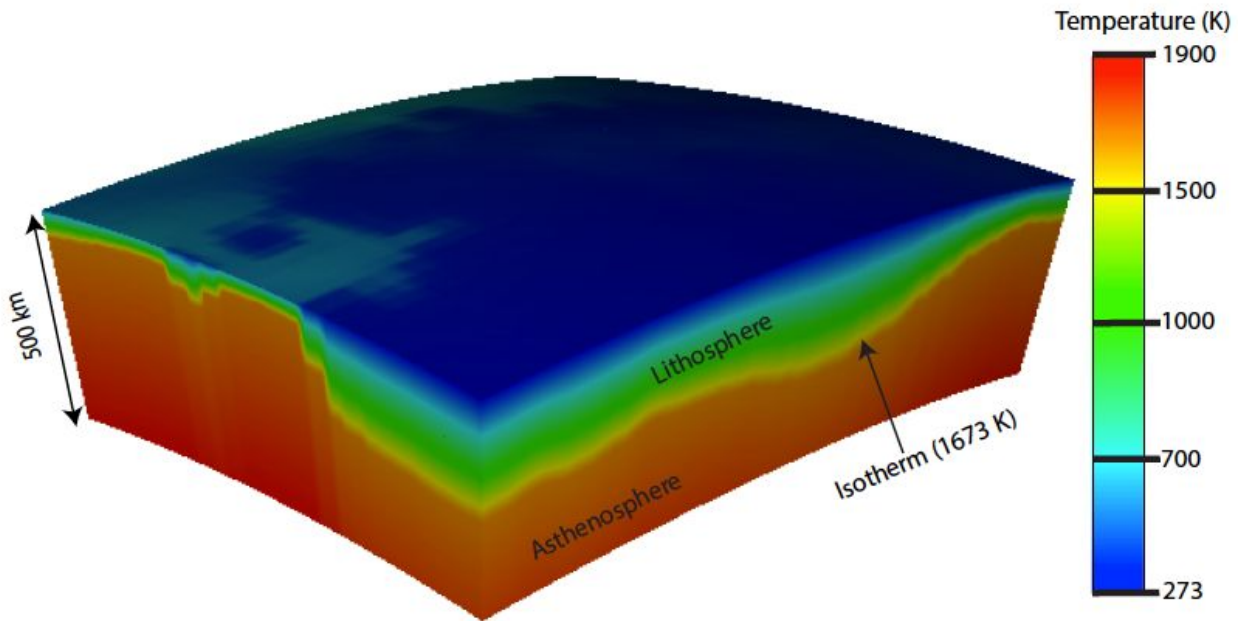
I created a new initial temperature condition that combines S40RTS and an ascii grid containing an upper mantle tomography. The data is read as Vs perturbations and is scaled to temperature using the functionality Jacky Austermann implemented for the S40RTS initial temperature condition (see “Implementation of a depth dependent shear wave to density scaling” above). There is an option to smooth the transition between the two tomographic models with a depth weighted combination of Vs in this region. I also implemented tests for this functionality. The model shown below is using Schaeffer and Lebedev (2013) Vs perturbations in the upper 700 km of the mantle.



A cookbook for the adiabatic boundary as initial temperature condition

Emmanuel Njinju

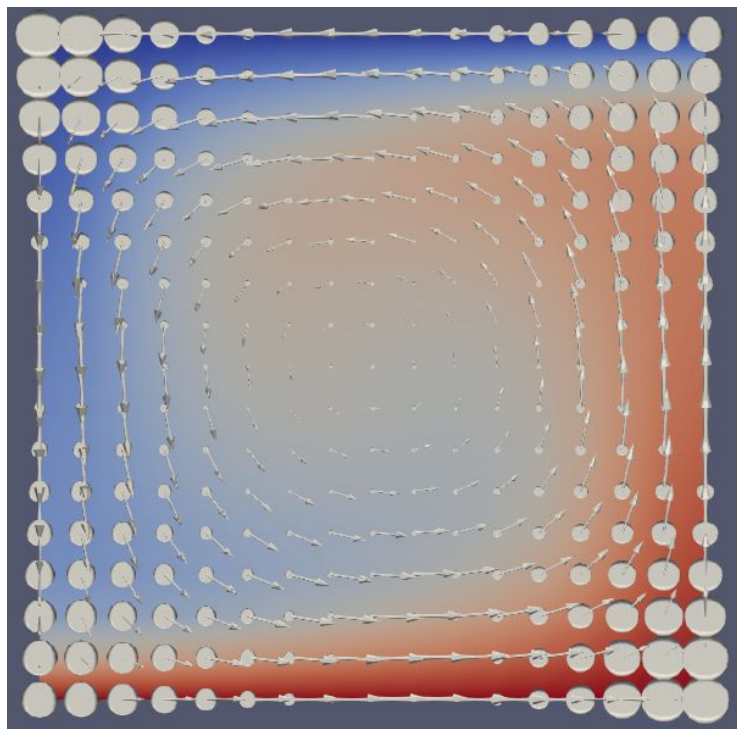
I wrote a cookbook that uses the adiabatic boundary plugin as initial temperature condition. This plugin allows for discretizing the model domain into layers separated by a user-defined isothermal boundary, which is an approximation for a thermal lithosphere. The geophysical set-up employs a table look-up approach, where the user defines the adiabatic boundary or lithospheric thickness in ASPECT as an input ASCII data file that is formatted as 3 columns of latitude, longitude and depth, where depth is in kilometers. The figure below is an initial temperature model highlighting the 1673.15 K temperature contour or adiabatic boundary, which marks the LAB corresponding to a sharp change in the geothermal gradient.



Visualization of the strain rate tensor

Bart Niday

Previously, ASPECT had no way to directly output the strain rate tensor for visualization - the “strain rate” plugin outputs the norm of the strain rate tensor, but the tensor itself had to be calculated in the visualization software. A new plugin, “strain rate tensor”, uses deal.II 9.0 functionality to output the full strain rate tensor in the visualization files.



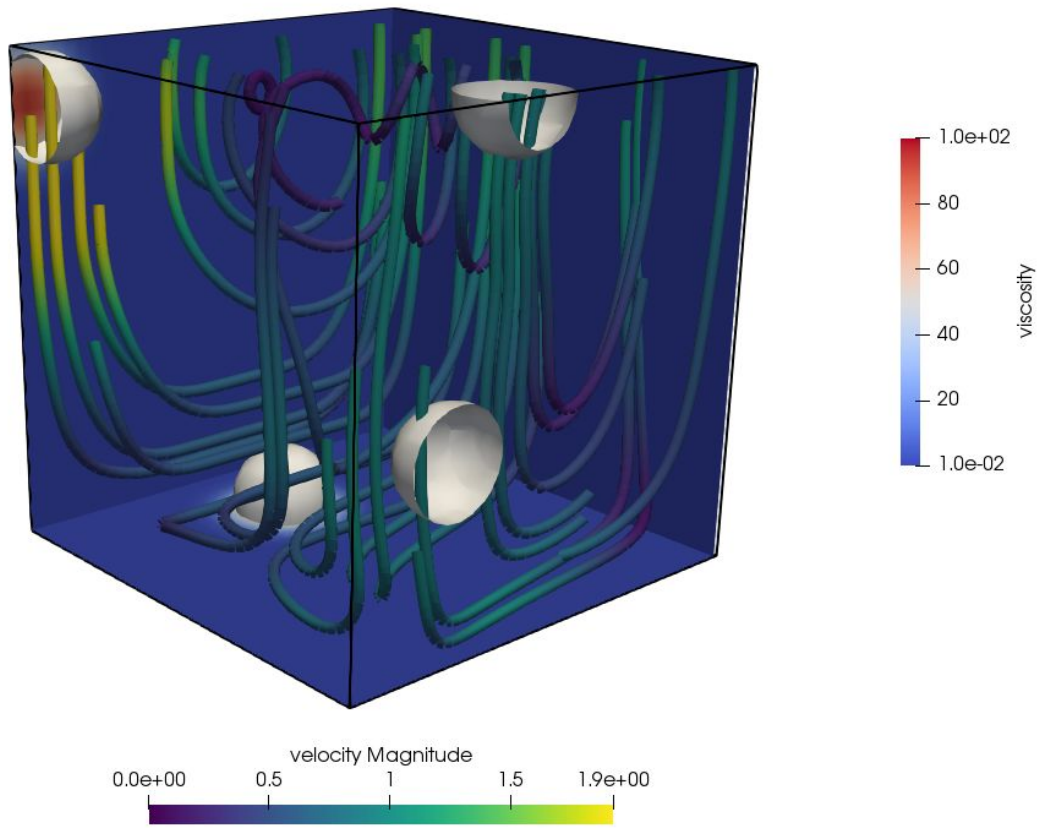
Implementation of the NSinker benchmark

Rene Gassmoeller, Cedric Thieulot, Conrad Clevenger, Timo Heister

We combined our preexisting implementations of the ‘NSinker’ benchmark as discussed in Rudi et al. (2017) and May et al. (2015) and created a preliminary cookbook for this benchmark that will be finished after the hackathon. The benchmark illustrates deficiencies of our current Schur complement preconditioner for distributed local viscosity contrasts and will be used as a starting point to benchmark better preconditioners as described in Rudi et al. (2017).

The table below shows the worst case scenario with no material model averaging. Rows show the number of sinkers and columns show the viscosity contrast between sinkers and surrounding material. The number in each cell shows the outer GMRES iterations for a single Stokes solve with the newly added .prm file of the benchmark. Empty cells mean the solver does not converge with our current preconditioner.

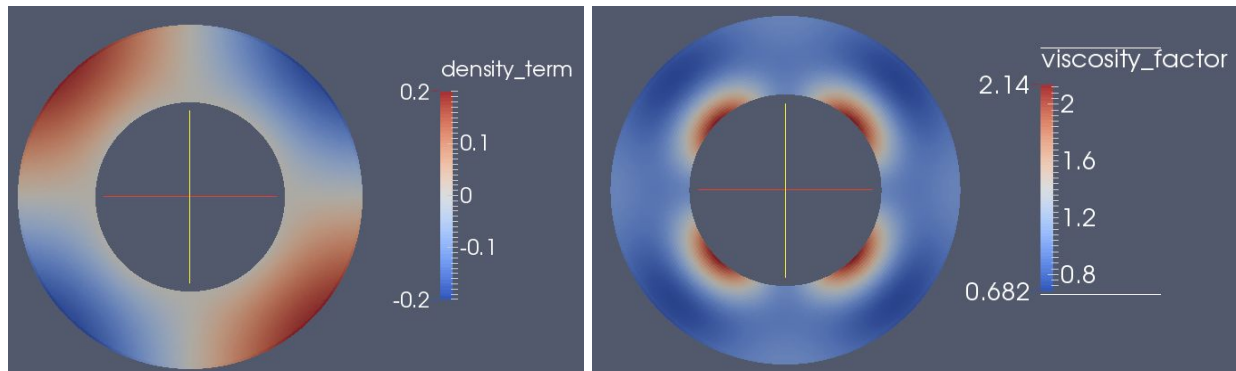
#sinkers/DR	1e4	1e6	1e8	1e10
1	22	35	78	164
4	31	62	161	341
8	41	87	204	
12	46	111	413	
16	69	199	827	
20	77	249	484	
24	78	255		
28	94	392		



Implementation of adjoint sensitivity kernels

Jacky Austermann

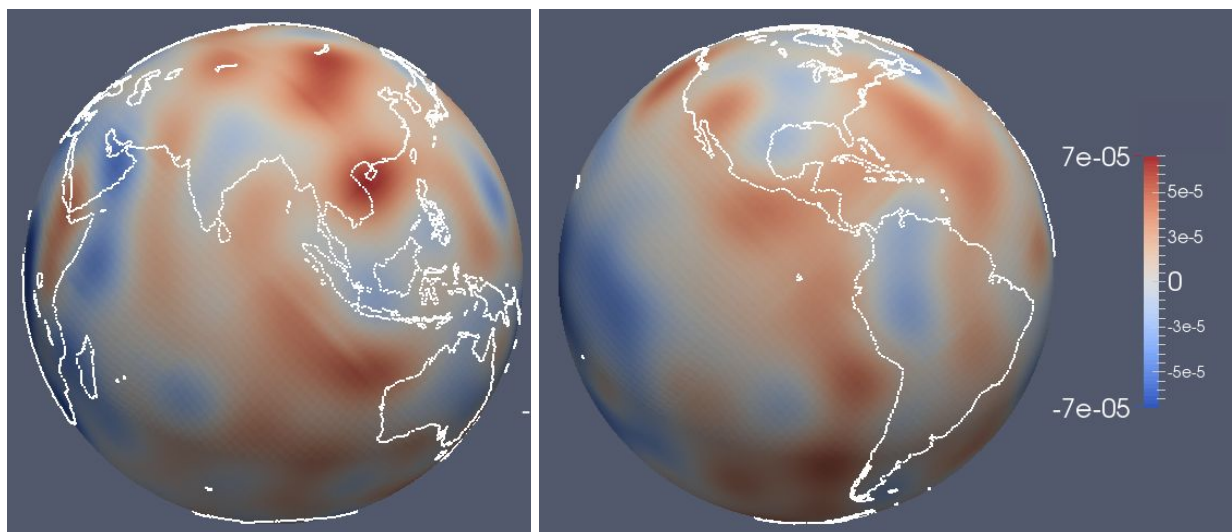
I've continued working on implementing the adjoint equations for the Stokes problem in ASPECT. There is now an adjoint solver scheme that solves the forward equations, adjoint equations, and sensitivity kernels. A figure of the sensitivity kernels for viscosity and density are shown below. This is for a run with a spherical hexagonal perturbation of degree 2. The sensitivity kernels are with respect to measuring the dynamic topography at the surface.



Calculation of gravity anomalies in geoid postprocessor

Jacky Austermann and Ludovic Jeanniot

We worked on extending the existing geoid postprocessor to also output radial gravity anomalies. This was done by taking the analytical derivative of the already computed gravity potential with respect to the radius. The gravity anomalies are outputted as visualization only, but an extension to write them out into an ascii file is easy to implement if needed. Since this approach uses spherical harmonics it is limited to the 3D spherical shell geometry model. The implementation has not been thoroughly tested / benchmarked yet, the pull request is therefore marked as Work in Progress. The figure shows gravity anomalies (in m/s²) at the surface as calculated with the S20RTS cookbook at a global refinement level 4. (The color scale corresponds to a range of -7mgal to +7mgal.)



Implementation of a depth-dependent initial temperature plugin

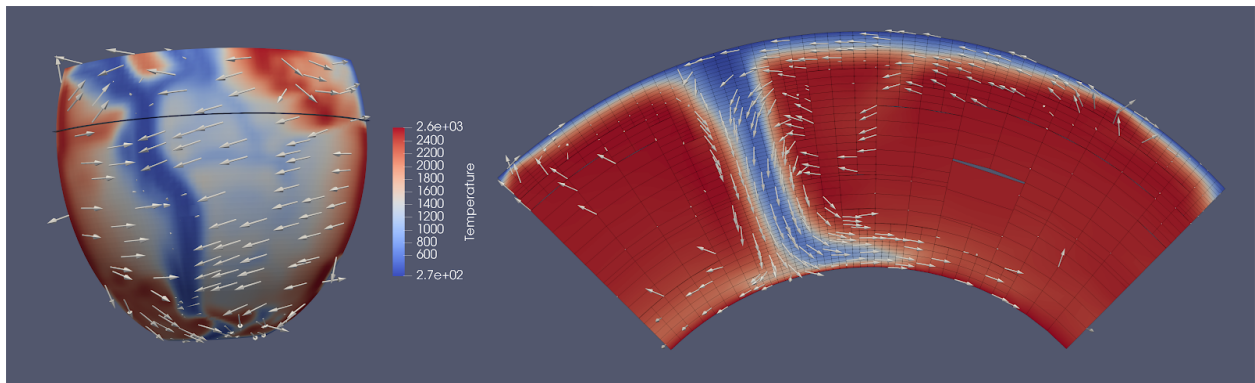
Marie Kajan

Many of the existing initial temperature plugins add temperature perturbations to a background temperature that is defined within the plugin. For example, the ‘S40RTS perturbation’ initial temperature adds tomography-based temperature perturbations to a single constant value called the ‘reference temperature,’ or to the adiabatic temperature profile calculated by ASPECT. Geodynamic models often use a depth-dependent temperature or geotherm. The ‘ascii profile’ initial temperature plugin allows a background temperature profile to be read in from an ASCII data file. This is designed to be combined with other models using the ‘List of model operators’ parameter to create composite initial conditions.

Set up a 3D subduction model for South America

Diandian Peng

Plate reconstruction models are important constraints for geodynamical simulation. In this project, I set up a 3D subduction model for South America with time-dependent velocity boundary conditions. Plate velocities which come from Matthews et al. (2016) are exported from GPlates. The region of this model is: longitude from 100°W to 10°W, latitude from 70°S to 20°N, depth from surface to core-mantle boundary. The subduction zone within the region is mainly the subduction of the Nazca plate under the South American plate. The model has a chunk geometry and a simple viscosity structure, which only depends on temperature. The model runs from 100 Ma to the present day. The figure below shows the result of this model at the present day. The left panel is the temperature at 160 km depth with velocities shown as arrows. The low temperature zone along the coastline of South America is due to the subducting Nazca slab. The black curve marks the position of the cross section on the right panel, which shows the temperature distribution, flow velocities and the mesh.



Parse map utility function

Paul Bremner

This is a new function in the utilities namespace that takes a string argument that is interpreted as a map with the form "key1 : value1, key2 : value2, etc", and then parses it to return a vector of these values where the values are ordered in the same way as a given set of keys. This function also has the ability to parse a simple list of comma separated values "value1, value2, value3, ..." (i.e., without the "keyx :" part) in the same order as provided. The function has an option to allow for a background field to be required, which is needed when dealing with compositional fields in material models. When using a map, the expected keyword for the background field is "background". The special keyword "all" assigns the associated value to all fields, including a background if required. This has been implemented in the multicomponent material model, and the picture below is a snippet of the multicomponent .prm file as a visual example:

LIST OF VALUES EXAMPLE:

```

subsection Material model
set Model name = multicomponent
subsection Multicomponent
  set Reference temperature = 0.0
  set Densities = 3300, 3200, 3600,3400
  set Specific heats = 1250
  set Thermal conductivities = 4.7
  set Thermal expansivities = 4e-5
  set Viscosities = 1.e21, 1.e20, 1.e23, 1.e22
  set Viscosity averaging scheme = geometric
end
end

```

MAP WITH KEYS EXAMPLE:

```

subsection Material model
set Model name = multicomponent
subsection Multicomponent
  set Reference temperature = 0.0
  set Densities = Crust:3200, UpperMantle:3600, LowerMantle:3400, bg:3300
  set Specific heats = all:1250
  set Thermal conductivities = all:4.7
  set Thermal expansivities = all:4e-5
  set Viscosities = bg:1.e21, Crust:1.e20, UpperMantle:1.e23, LowerMantle:1.e22
  set Viscosity averaging scheme = geometric
end
end

subsection Compositional fields
set Number of fields = 3
set Names of fields = Crust, UpperMantle, LowerMantle
end

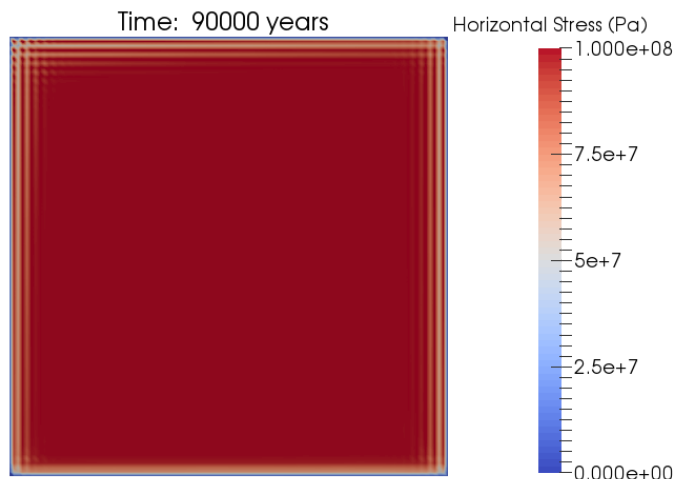
```

Implementing a viscoelastic-plastic rheology

John Naliboff

I combined functionality from the viscoelastic and visco_plastic material models in a new material model named viscoelastic_plastic. This material model can be applied to a wide range of lithospheric deformation problems, which commonly involve a range of deformation mechanisms including non-linear viscous flow, plasticity and viscoelastic flexure. This material includes two benchmarks, which examine an analytical solution for viscoelastic-plastic stress build-up or development of viscoelastic-plastic shear bands.

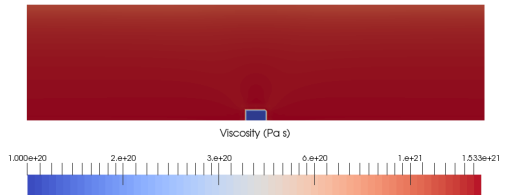
The image below shows the results of an experiment based on an analytical solution for viscoelastic stress build-up with a plastic yield criterion of 100 MPa. Without an imposed yield stress, the viscoelastic stresses would quickly build up to 200 MPa (exceed 100 MPa after ~30 kyr). The image shows the maximum horizontal stress state is clearly capped at 100 MPa in the model (e.g., away from edge boundary oscillations), even after 90 kyr of deformation.



The images below shows development of visco-elastic plastic shear bands in a setup very similar to the one outlined by Kaus, 2010 (Tectonophysics). The experiment imposes a background strain-rate (extensional) of 1e-15 in a viscoelastic-plastic medium containing a small

weak viscous inclusion at the model's bottom center. In contrast to a visco_plastic rheology, plastic shear bands develop overtime as the viscoelastic stresses buildup and eventually reach the plastic yield strength. This is illustrated in the images below, which show the viscosity structure after 1 and 20 thousand years of deformation.

Time: 1000.0 years

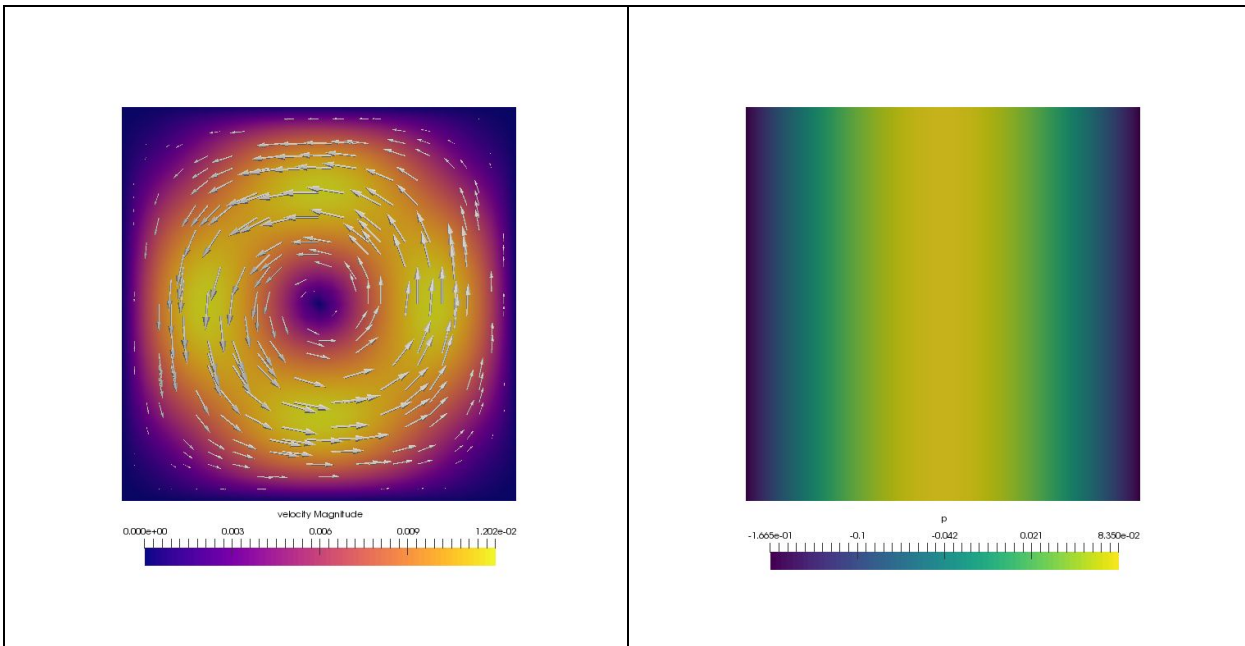


f

2D analytical benchmark, part 1

C. Thieulot

This benchmark is taken from the FEM book of Donea & Huerta. The domain is a unit square, density and viscosity are 1, but the gravity vector components gx and gy are complicated 5th order polynomials of the spatial coordinates x and y . The velocity field resembles a convection cell, while the pressure is a parabola.

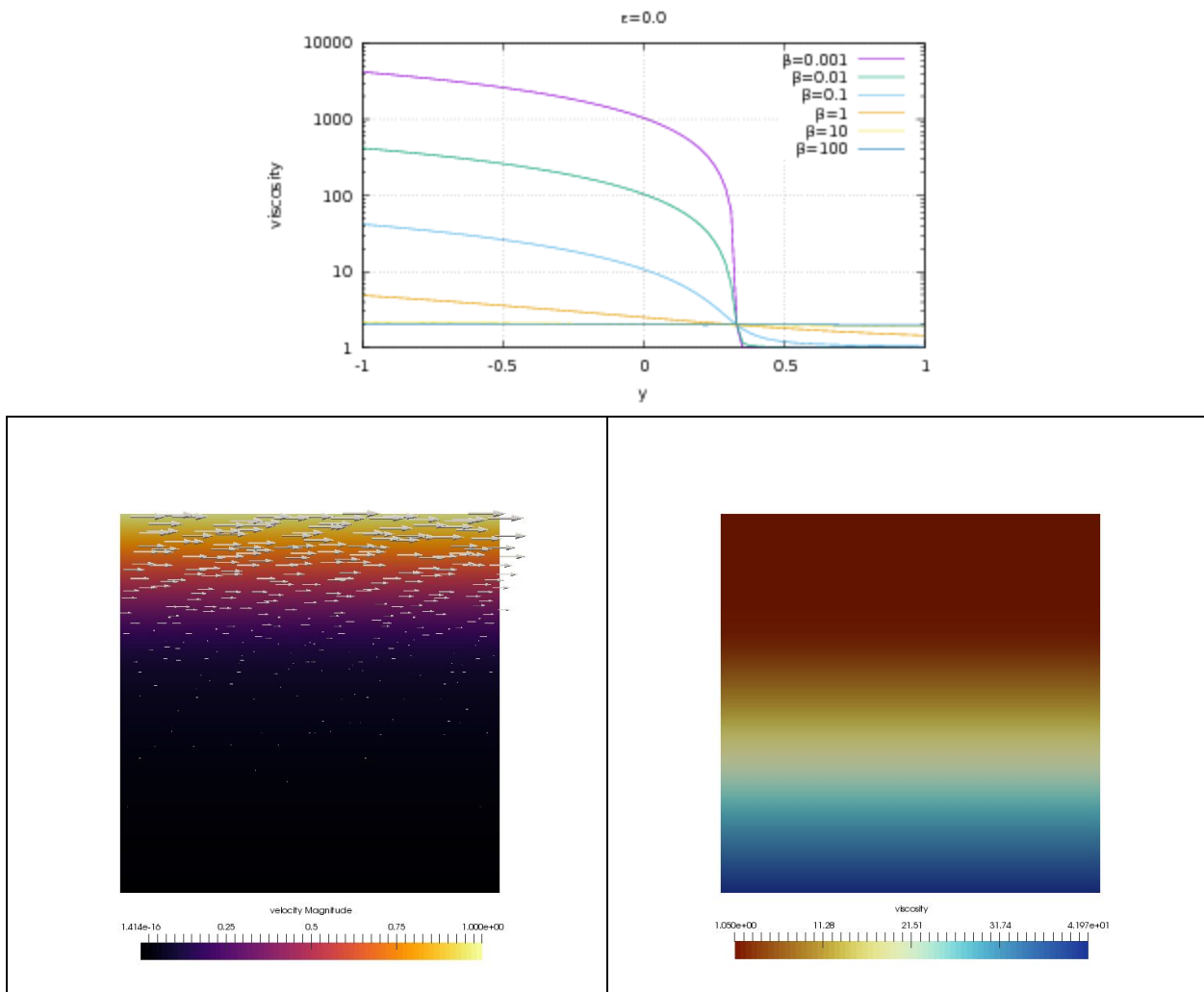


2D analytical benchmark, part 2

C. Thieulot

The idea behind this alternate benchmark is to construct an analytical solution to the incompressible Stokes equation in the case where the viscosity field showcases a contrast at a chosen location $y = y_0$, for which amplitude and width can be controlled. This is useful for testing discretizations of problems in which the viscosity is expected to have large variations, possibly within individual cells.

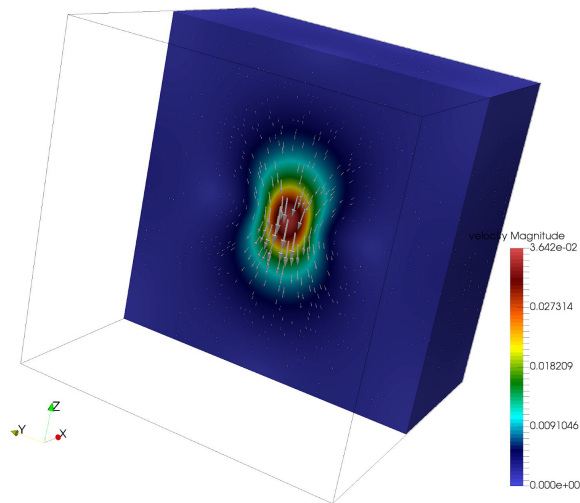
The figure below shows preliminary results for this benchmark.



Implementation of stabilised Q1Q1 element

C. Thieulot & W. Bangerth

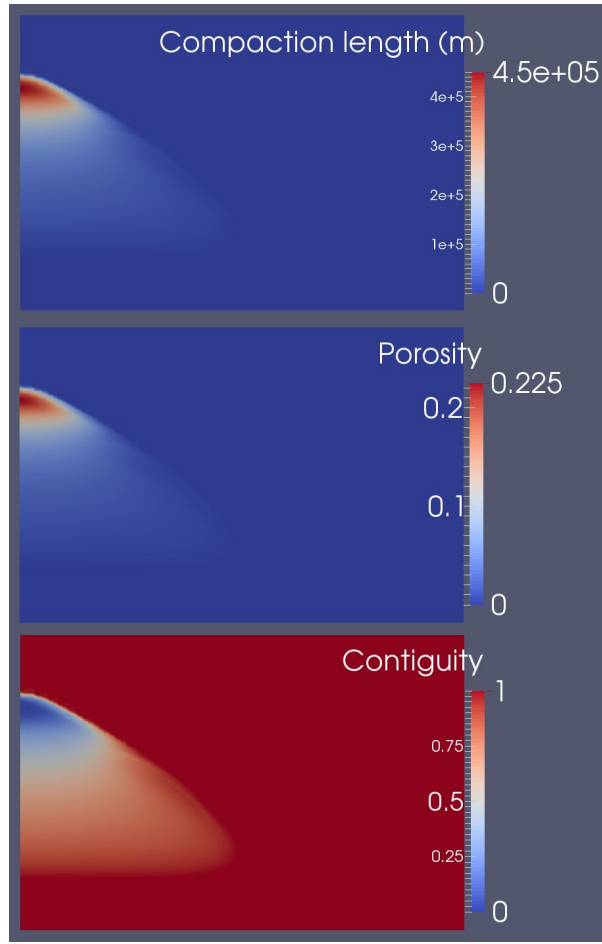
A preliminary implementation of this element is now present in a branch. Several encouraging tests have been carried out, such as the 3D Stokes sphere.



Implement new properties in the visualization for melt material properties

Joe Schools

I added a visualization for compaction length, the fundamental length scale of fluid-matrix interaction, into the existing melt material properties visualization postprocessor. Additionally, I implemented a visualization for contiguity, a property related to porosity, which is a measure of how the grains of the solid matrix are touching.



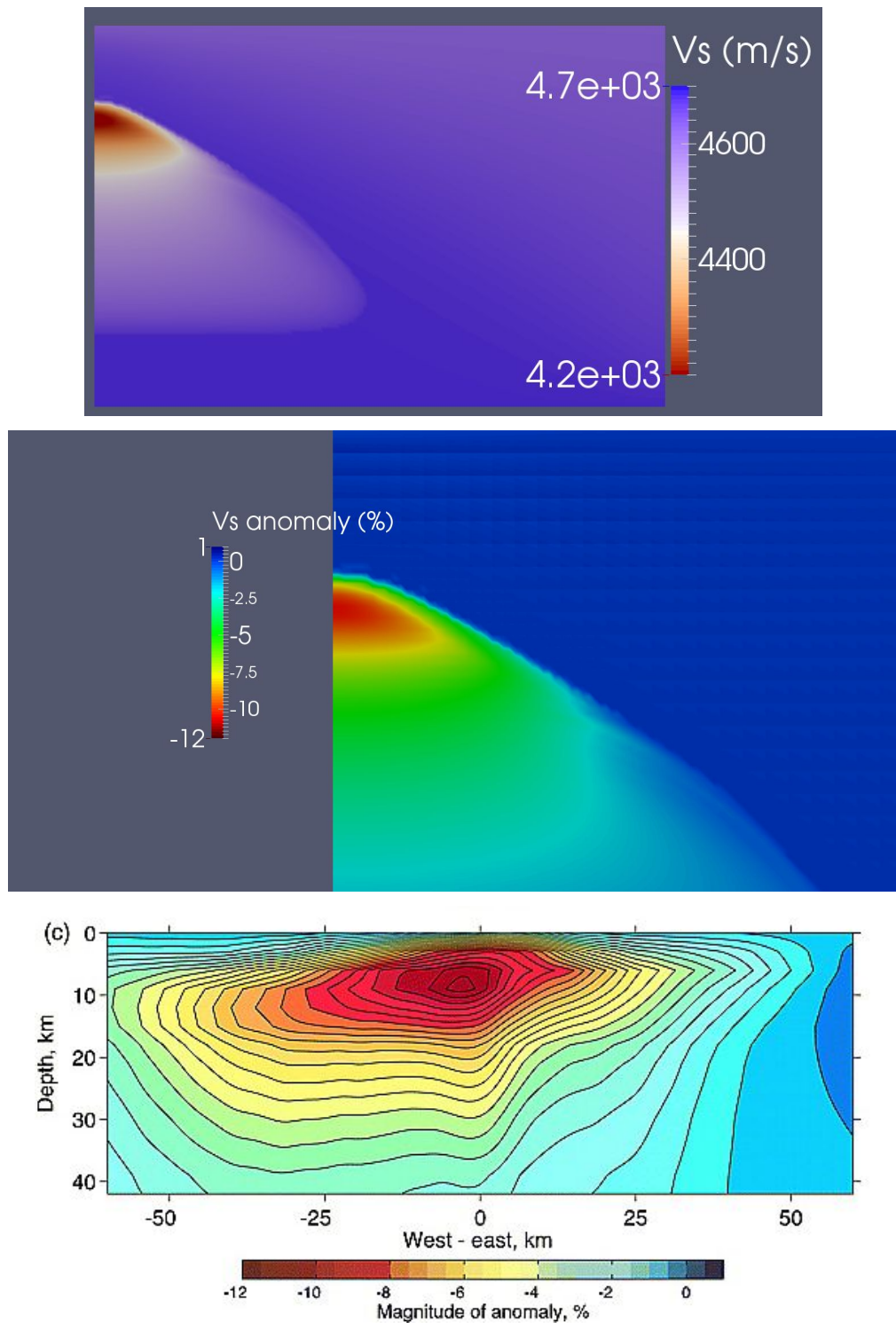
The implemented calculation for contiguity is dependent on the porosity, and is used to calculate the seismic velocities described in the next section.

New postprocessor plugin to calculate the seismic velocities and velocity anomalies in models with melt

Joe Schools

Using a self consistent set of equations, the seismic velocities (V_p , V_s) in models involving melt (or any model with a porosity field) are calculated based on user input of bulk moduli of the solid and liquid, shear moduli of the solid, and Poisson ratio, and the model output of porosity and density. Additionally the plugin can calculate V_p and V_s anomalies compared to velocities ignoring melt to see the contribution of melt to the seismic profile. The images below are computed using the new functionality when applied to the mid-ocean ridge cookbook. The third figure from Dunn and Forsyth (2003) shows a tomographic image of the East Pacific Rise for comparison.

Future work may involve using a lookup table for the moduli and Poisson ratio values, instead of using a constant user input value.



New postprocessor to compute gravity acceleration and potential

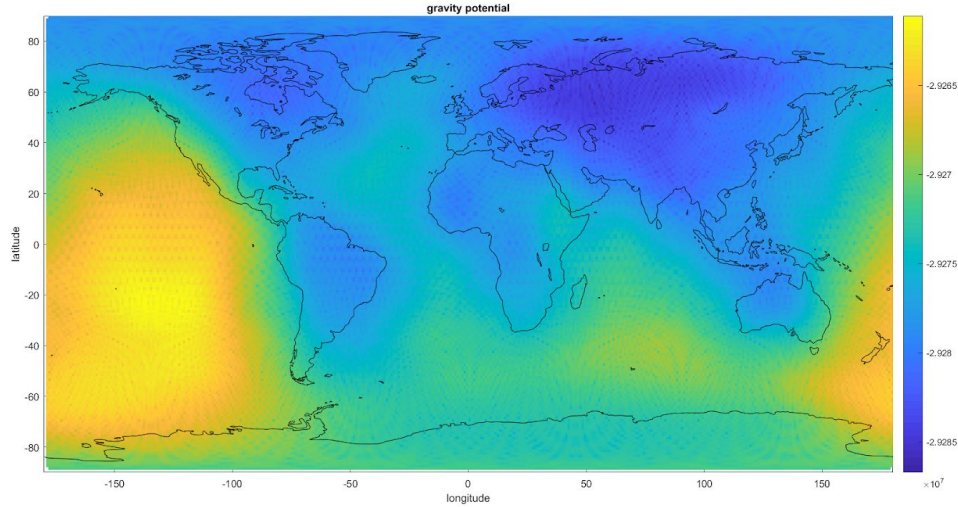
Ludovic Jeanniot, John Naliboff, and Cedric Thieulot

This new postprocessor computes gravity acceleration and gravity potential for a set of points (e.g. satellites) in or above the model surface for a user-defined range of latitudes, longitudes

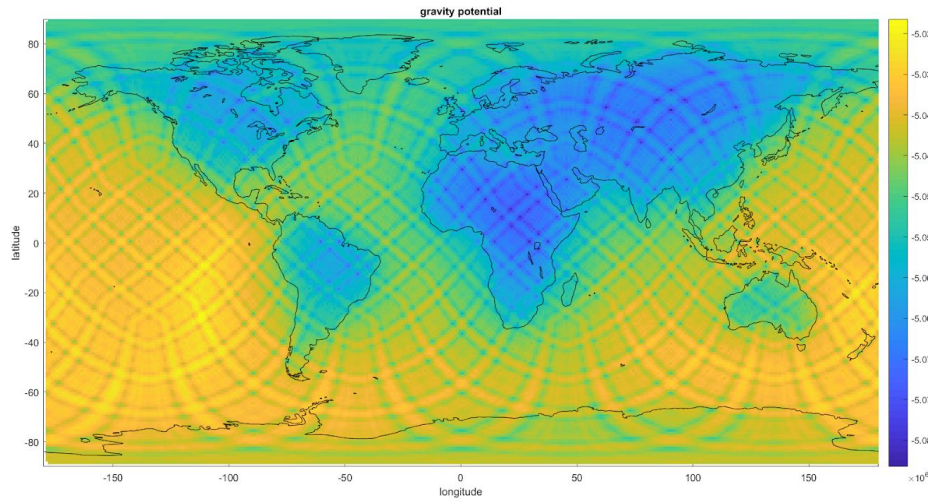
and radii. The method we use here is an integration of the density of the domain. The post-processor receives as arguments the coordinates $r'=(x,y,z)$ of a point and returns the gravity vector components $g=(g_x, g_y, g_z)$ at this location by means of:

$$g(r') = \int_{\Omega} G \frac{\rho(r) - \rho_0}{|r' - r|^3} (r' - r) d\Omega$$

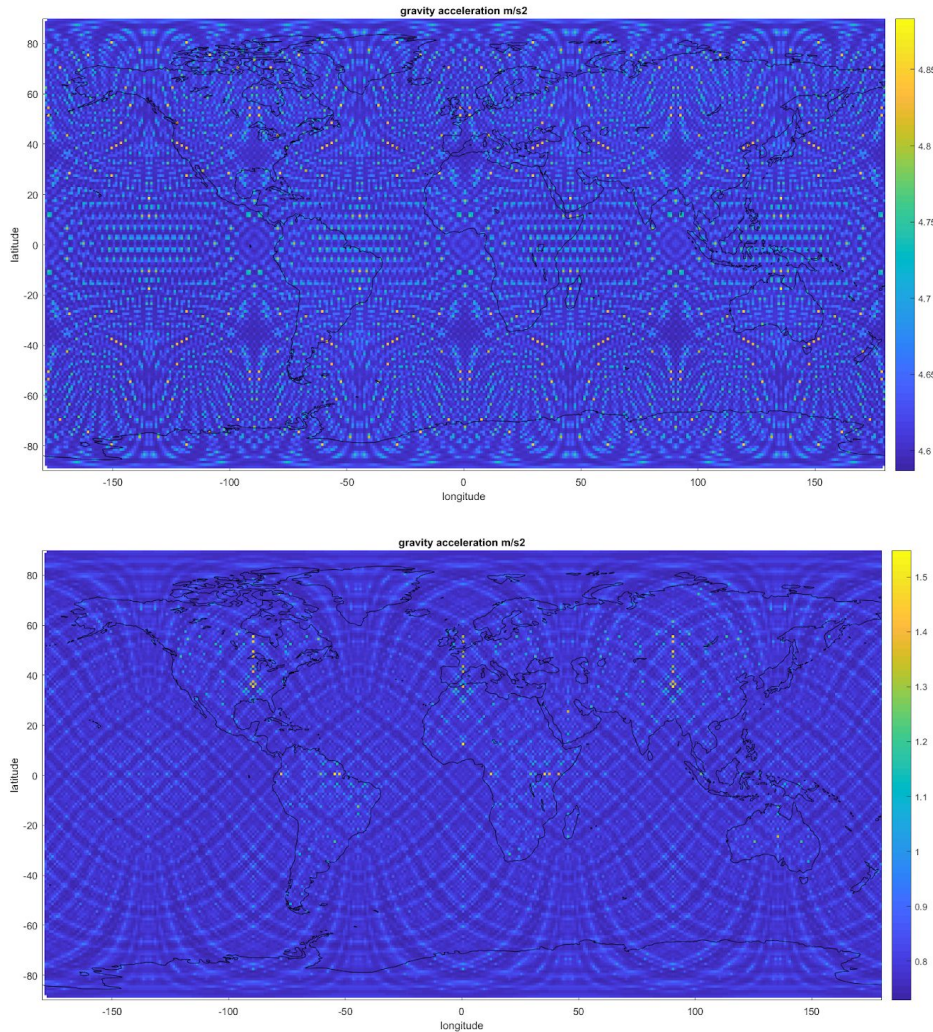
We tested the gravity post-processor on S40RTS and Crust1.0 using a spherical shell. Crust1.0 was uploaded in ASPECT and should become a new material model soon. The idea is to later couple S40RTS and Crust1.0 in one model and predict gravity acceleration and potential:



Gravity potential using S40RTS for the whole mantle from CMB to 300 km depth with a global mesh refinement level 3 and additional local mesh refinement level 5 near the surface.



Gravity potential using crust1 in the upper asthenosphere (300 km depth) to lithosphere with a global mesh refinement level 2 and additional local mesh refinement level 4 for the crust.



Gravity acceleration using S40RTS (upper figure) or Crust1.0 (lower figure). As the gravity field is the spatial derivative of the potential, gravity becomes more sensitive to grid resolution. A solution to this problem requires a significantly higher level of refinement, globally and specifically locally at the surface.

Speed up the assembly for the Newton solver

Menno Fraters and Rene Gassmoeller

We noticed before the hackathon that the assembly of the Newton solver was very slow. During the hackathon we profiled the corresponding functions and identified some slow code which could be significantly optimized. Before the optimization for difficult problems we spent more than 50% of the walltime in the assembly of the Newton solver:

Section	no. calls	wall time	% of total
Total wallclock time elapsed since start		1.16e+05s	
Assemble Stokes system	351	425s	0.37%
Assemble Stokes system newton	7304	6.47e+04s	56%
Assemble Stokes system picard	748	1.55e+03s	1.3%
Assemble Stokes system rhs	7701	3.15e+03s	2.7%
Assemble composition system	8052	4.13e+03s	3.6%
Assemble temperature system	8052	5.47e+03s	4.7%
Build Stokes preconditioner	8052	2.11e+04s	18%
Build composition preconditioner	8052	559s	0.48%
Build temperature preconditioner	8052	474s	0.41%
Solve Stokes system	8052	1.22e+04s	11%
Solve composition system	8052	324s	0.28%
Solve temperature system	8052	306s	0.26%
Free surface	352	117s	0.1%
Initialization	1	1.19s	0%
Postprocessing	351	77.5s	0%
Refine mesh structure, part 1	352	139s	0.12%
Refine mesh structure, part 2	352	48.9s	0%
Setup dof systems	353	225s	0.19%
Setup initial conditions	2	2.08s	0%

So we ran a smaller test and our initial output for that test was:

Section	no. calls	wall time	% of total
Total wallclock time elapsed since start		88.6s	
Assemble Stokes system	1	1.66s	1.9%
Assemble Stokes system Newton	4	16.8s	19%
Assemble Stokes system Picard	3	7.36s	8.3%
Assemble Stokes system rhs	6	5.07s	5.7%
Assemble temperature system	7	12.5s	14%
Build Stokes preconditioner	7	19.5s	22%
Solve Stokes system	7	12.6s	14%
Initialization	1	5.7s	6.4%
Postprocessing	1	2.55s	2.9%
Setup dof systems	1	0.887s	1%
Setup initial conditions	1	1.24s	1.4%

After the improvements it became:

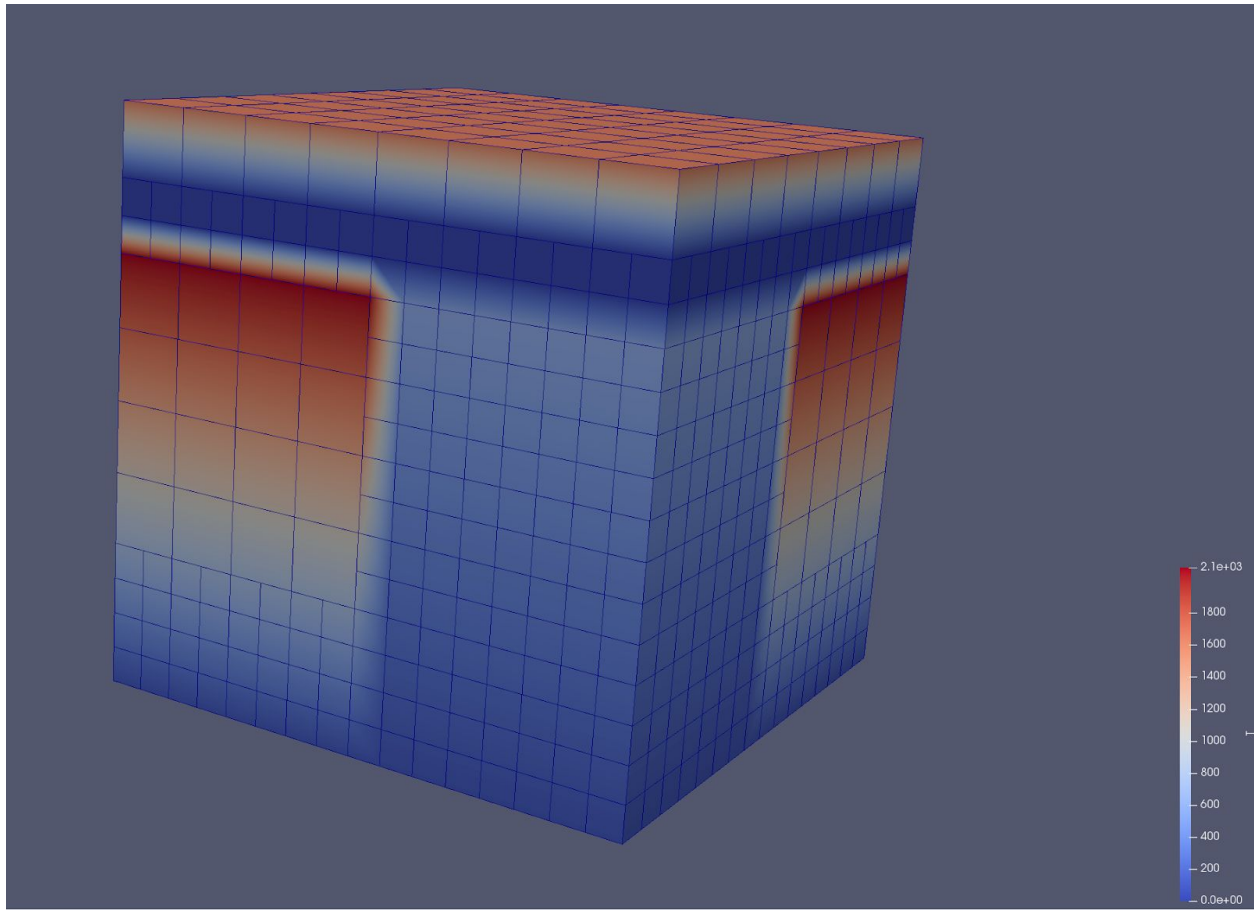
Section	no. calls	wall time	% of total
Total wallclock time elapsed since start		69.1s	
Assemble Stokes system	1	1.35s	2%
Assemble Stokes system Newton	4	8.95s	13%
Assemble Stokes system Picard	3	4.09s	5.9%
Assemble Stokes system rhs	6	4.49s	6.5%
Assemble temperature system	7	10.9s	16%
Build Stokes preconditioner	7	15.6s	23%
Solve Stokes system	7	12s	17%
Initialization	1	5.3s	7.7%
Postprocessing	1	2.25s	3.3%
Setup dof systems	1	0.779s	1.1%
Setup initial conditions	1	0.987s	1.4%

Which is nearly a speed up of two for both the Newton and Picard assembly.

Added test for the isotherms pull request

Menno Fraters

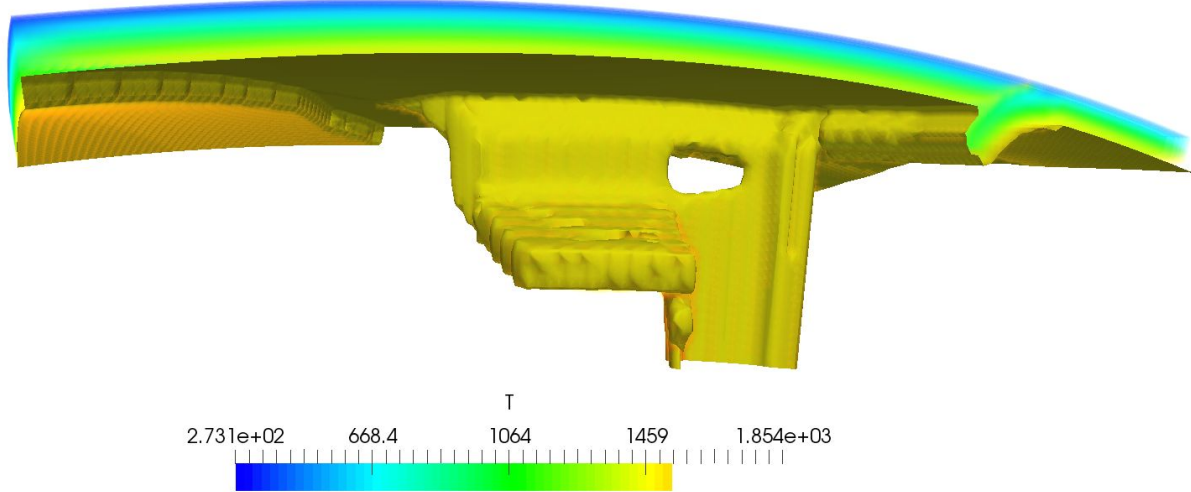
The already existing pull request for adding a isotherms mesh refinement criterion has been looked at again, and requires a bit of rewriting. To make sure the results stay the same during the rewrite, a test has been added to check this.



World builder structure

Menno Fraters

I worked on defining the exact structure of the world builder, a module that can create complex initial conditions as they usually exist at plate boundaries on Earth, and we decided to separate it from ASPECT so that other geodynamics codes beside ASPECT can also make use of it. It will for now remain part of the ASPECT repository as a submodule. Here is a figure of a complex subduction zone including slab holes and slab tear that was generated with the world builder:



Tracking the plastic and/or viscous strain

Anne Glerum

The visco-plastic material model now includes functionality to track either the total strain or the plastic and/or viscous strain. These strains are then used to linearly weaken the plastic (cohesion and internal angle of friction) and viscous (prefactor) rheological parameters. Also, additional material output is produced that shows which regions are plastically yielding (see figure below).

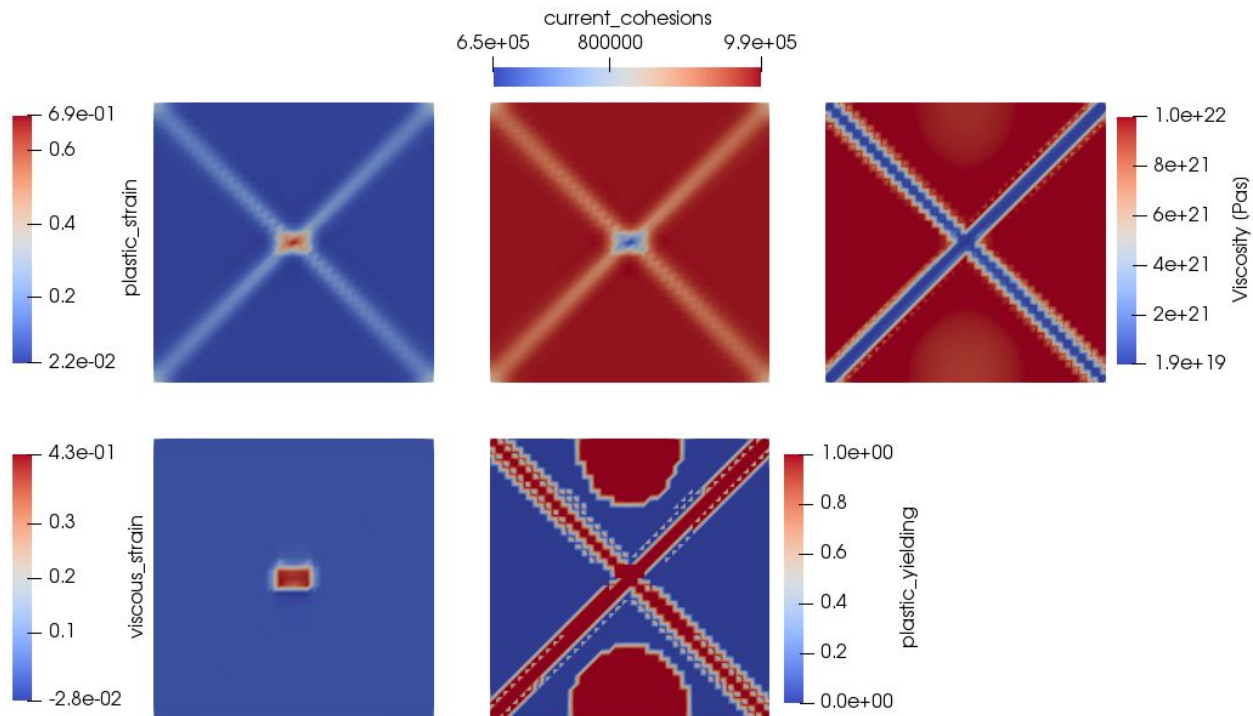


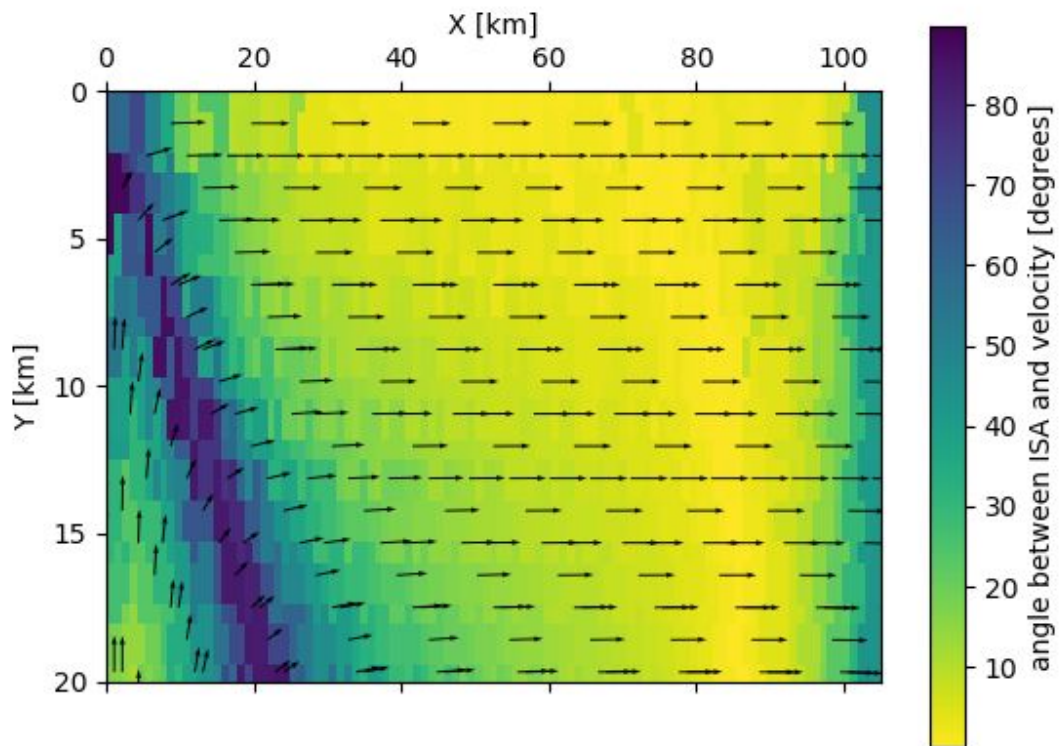
Figure: Plastic strain, cohesion, viscosity, viscous strain and plastic yielding for the visco_plastic_yield_plastic_viscostrain_weakening test after 5.3 My. Where the viscous

stress exceeds the yield stress, plastic yielding occurs. Here plastic strain is accumulated, while everywhere else, viscous strain accumulates. The material's cohesion and internal angle of friction are subsequently weakened with the tracked plastic strain, while the viscous strain is used to weaken the dislocation creep prefactor. The resultant viscosity field reflects this.

Postprocessor to calculate the grain orientation lag parameter

Hannah Mark

I wrote a postprocessor which calculates and outputs the two quantities needed to calculate the grain orientation lag parameter described by Kaminski and Ribe (2002); namely, the angle between the infinite strain axis and the velocity (theta), and the timescale for the rotation of grains toward the ISA (τ_{ISA}). The figure below shows the angle theta calculated for a simple steady-state half mid-ocean ridge, forced by plate motion to the right on the top boundary, overlain with velocity vectors.



Option to skip solvers and initial conditions during pre-refinement

Ludovic Jeanniot and Wanying Wang

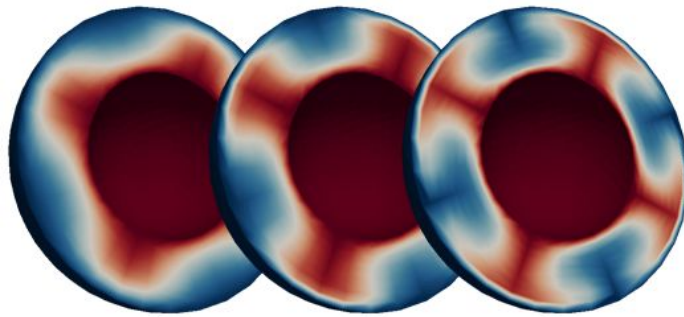
Using one or more initial adaptive refinement steps includes the setup of initial conditions, solution of the problem, and mesh refinement and repartitioning until the mesh is refined as desired and the main time loop can begin. For some model setups this initial phase of pre-refinement can take a long time when the initial condition is expensive to compute. Moreover, it is not necessary if the adaptive refinement is independent of the solution (e.g. spatial refinement to a specific area), because then the solution is not needed to begin the next refinement cycle. In order to avoid this wasted time, we added two input parameters in the subsection “Mesh refinement” that allow to skip the solvers or the initial condition setup (or both) during pre-refinement. As shown below, we compared the total time required for the computation of a 3D spherical instantaneous flow model with density structure and viscosity variations. The new options save 75% of the computing time:

Total wallclock time elapsed since start		2.03e+03s	
<hr/>			
Section	no. calls	wall time	% of total
+-----	+-----	+-----	+-----
Assemble Stokes system	5	107s	5.3%
Assemble composition system	5	31.4s	1.5%
Assemble temperature system	5	57.2s	2.8%
Build Stokes preconditioner	5	67.5s	3.3%
Build composition preconditioner	5	3.81s	0.19%
Build temperature preconditioner	5	3.79s	0.19%
Solve Stokes system	5	242s	12%
Solve composition system	5	1.49s	0%
Solve temperature system	5	1.61s	0%
Initialization	1	9.18s	0.45%
Postprocessing	1	444s	22%
Refine mesh structure, part 1	4	3.3s	0.16%
Refine mesh structure, part 2	4	13.7s	0.68%
Setup dof systems	5	11.1s	0.55%
Setup initial conditions	5	823s	41%
+-----	+-----	+-----	+-----
Total wallclock time elapsed since start		520s	
<hr/>			
Section	no. calls	wall time	% of total
+-----	+-----	+-----	+-----
Assemble Stokes system	1	15.7s	3%
Assemble composition system	1	4.99s	0.96%
Assemble temperature system	1	9.01s	1.7%
Build Stokes preconditioner	1	13.1s	2.5%
Build composition preconditioner	1	0.652s	0.13%
Build temperature preconditioner	1	0.655s	0.13%
Solve Stokes system	1	85.9s	17%
Solve composition system	1	0.456s	0%
Solve temperature system	1	0.503s	0%
Initialization	1	4.45s	0.86%
Postprocessing	1	210s	40%
Refine mesh structure, part 1	4	2.22s	0.43%
Refine mesh structure, part 2	4	7.28s	1.4%
Setup dof systems	5	6.9s	1.3%
Setup initial conditions	1	120s	23%
+-----	+-----	+-----	+-----

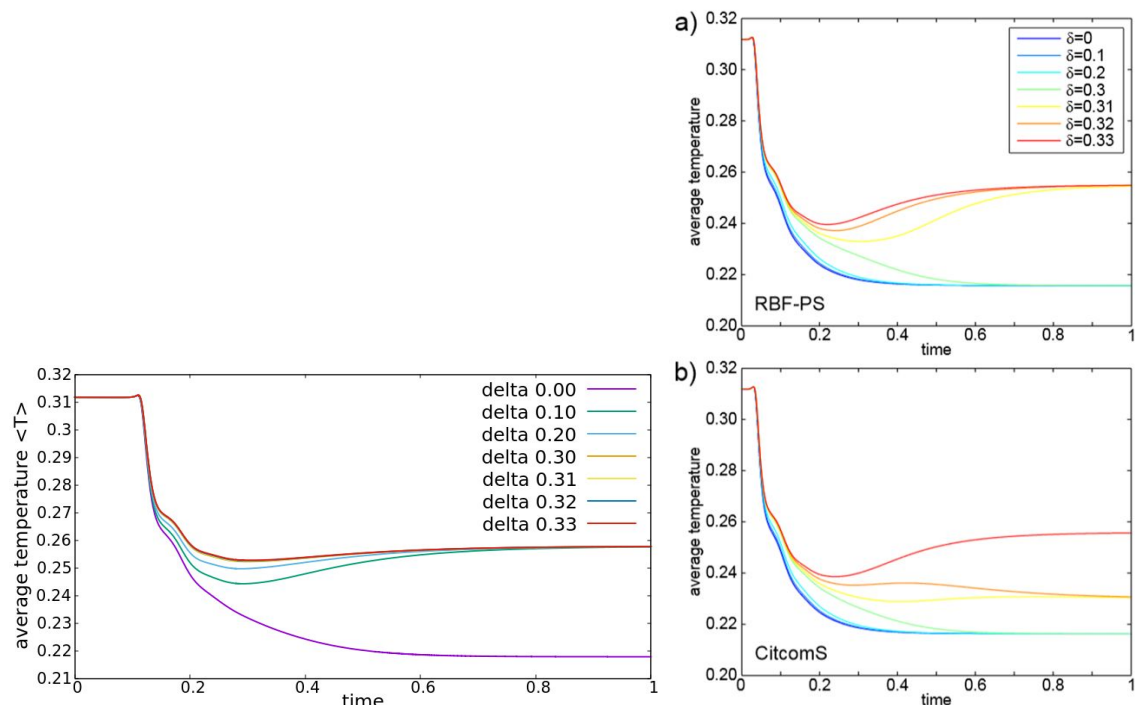
3D thermal convection benchmark in a spherical shell by Arrial et al. 2014

Ludovic Jeanniot and Cedric Thieulot

We are writing a benchmark on 3D thermal convection in a spherical shell based on the Arrial et al. (2014) benchmark using CitcomS. A plugin has been written based on the harmonic perturbation initial temperature already implemented in ASPECT. For our case, the perturbation has a cubic initial temperature profile (as shown in the figure below) that requires both an axisymmetric and nonaxisymmetric perturbation.



Thermal convection in a spherical shell. For the benchmark, this figure has to be changed to show not only the axisymmetric perturbation, but also the nonaxisymmetric one. (Red is hot, blue is cold.)



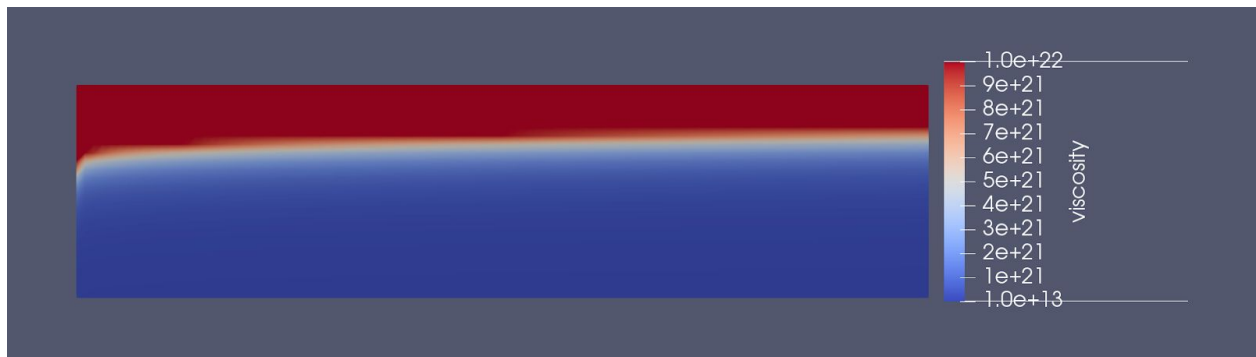
The delta factor affect the nonaxisymmetric perturbation by slowing it down with increasing delta. Here we show the resulting effect of delta on the average temperature and compared ASPECT (left) with numerical code CitcomS (a) and spectral RBF-PS model (b). The difference between ASPECT and the other models is due to a low resolution (level 3). Using a resolution level 4 in ASPECT show identical results to CitcomS.

A cookbook for convection on icy satellites

Jonathan Kay

I worked on implementing a cookbook for a viscoplastic ice model with diffusion creep. This model aims to build on the development previously done within ASPECT, but extend it to more

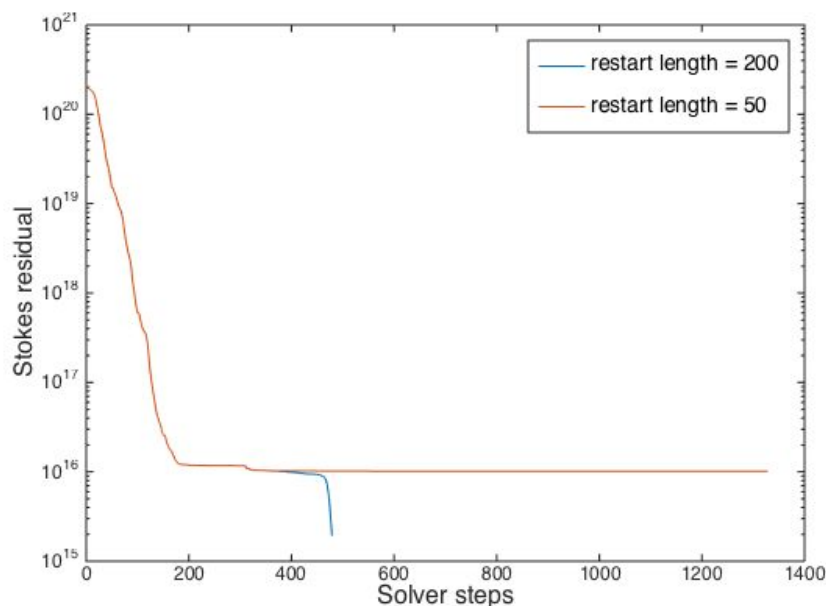
material parameters. In addition, this model implements the boundary heat flux model that allows the user to establish the heat flux through any boundary.



Testing new ‘GMRES solver restart length’ parameter

Marie Kajan

Strong viscosity contrasts can be difficult to implement in ASPECT due to convergence problems in the Stokes solver. This is even more true for lateral viscosity variations in 3-D spherical geometry. The new ‘Solver parameters/Stokes solver/GMRES solver restart length’ parameter allows users to adjust the number of iterations before the GMRES solver is reset. For more complicated models, this restart can occur prematurely such that the solver never converges given a specified error tolerance. The default value for the restart length is 50, however increasing this value increases the memory usage of the Stokes solver and makes each Stokes solve more computationally expensive. In my model, a viscosity field was imposed with radial and lateral variations of 5-7 orders of magnitude across a 3-D spherical shell domain. The default restart length of 50 did not converge, however setting the parameter to 200 allowed the solver to converge within 170 steps as shown in the convergence history below.

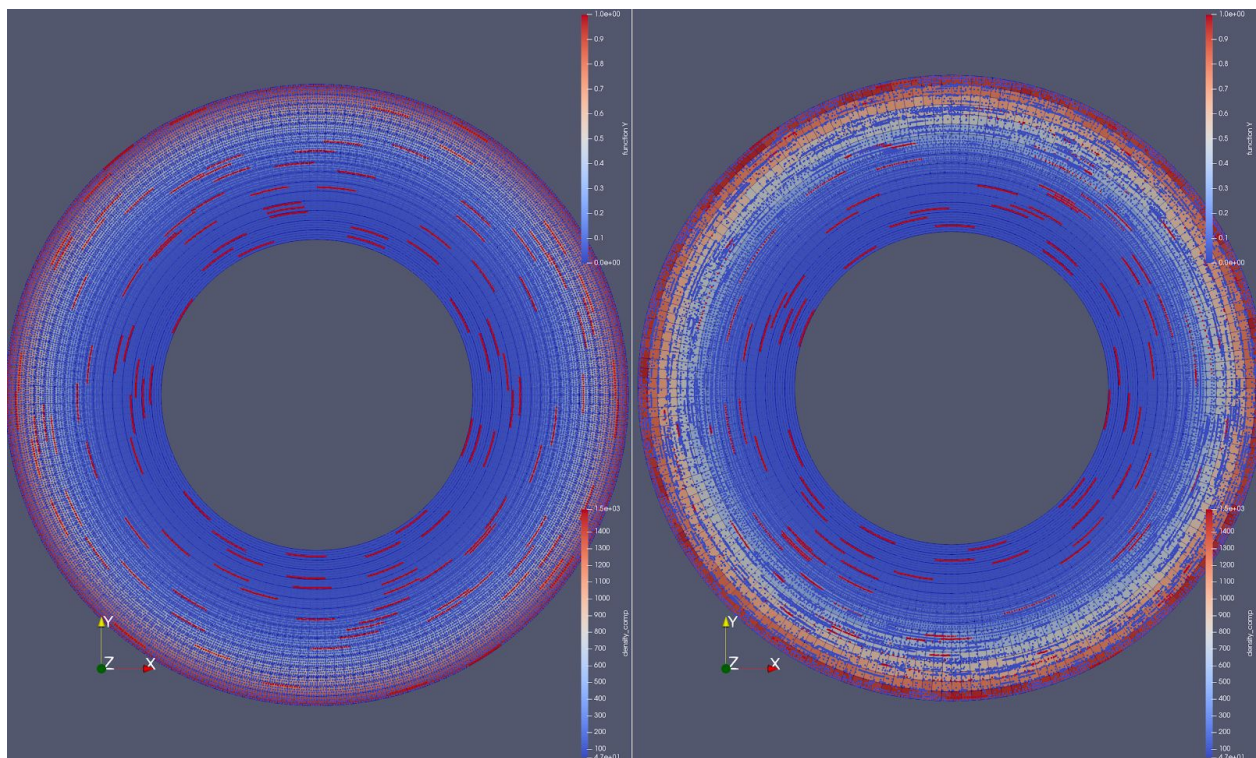


The result of increasing the input value for the new ‘GMRES solver restart length’ parameter in a model with high viscosity contrasts. The default value of 50 (shown in orange) results in non-convergence of the Stokes solver, but increasing this value to 200 (shown in blue) allows the solver to converge.

Development of a benchmark for active tracer particles in ASPECT

Gerry Puckett

This benchmark was developed in collaboration with Harsha Lokavarapu, who did not attend the Hackathon. The (ongoing) analysis of the results was being conducted in collaboration with Rene Gassmoller, Timo Heister and Wolfgang Bangerth. Some of this analysis was done at the Hackathon.



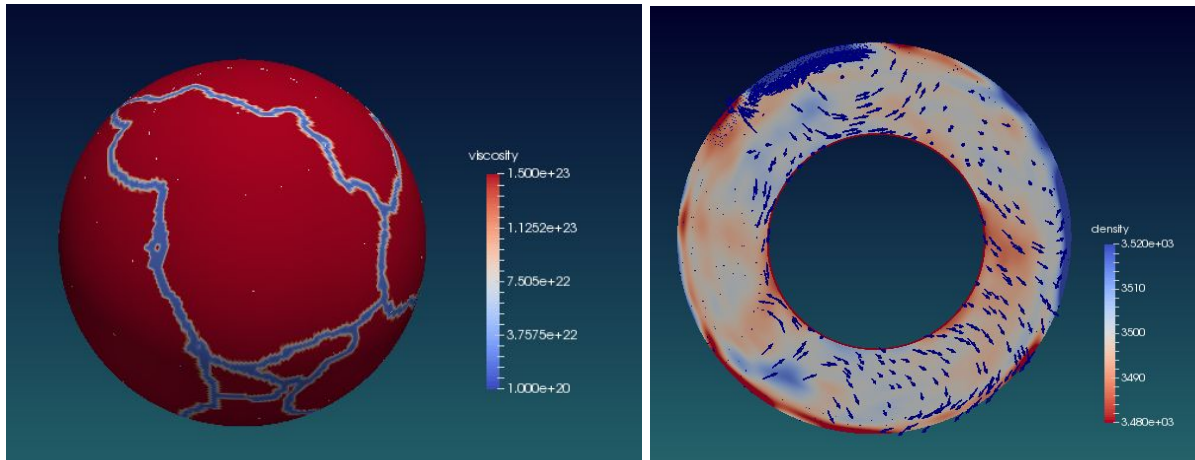
Two computations of a radial solution to the incompressible Stokes equations on the annulus $1 \leq r \leq 2$ in which the density is carried on particles that travel on concentric circles with a speed that increases monotonically as r increases from 1 to 2. The velocity and pressure are discretized with the Q_2 x Q_1 finite element combination and the particle positions are updated in time with a second order Runge-Kutta method. Initially there are $16 = 4 \times 4$ particles per cell. On the left we have interpolated the value of the density from the particles onto the finite element discretization of the Stokes equations with a (least-squares) bilinear interpolation method while on the right we have taken the arithmetic average of the particles in each cell and interpolate that value onto the finite element discretization. These images are at the time at

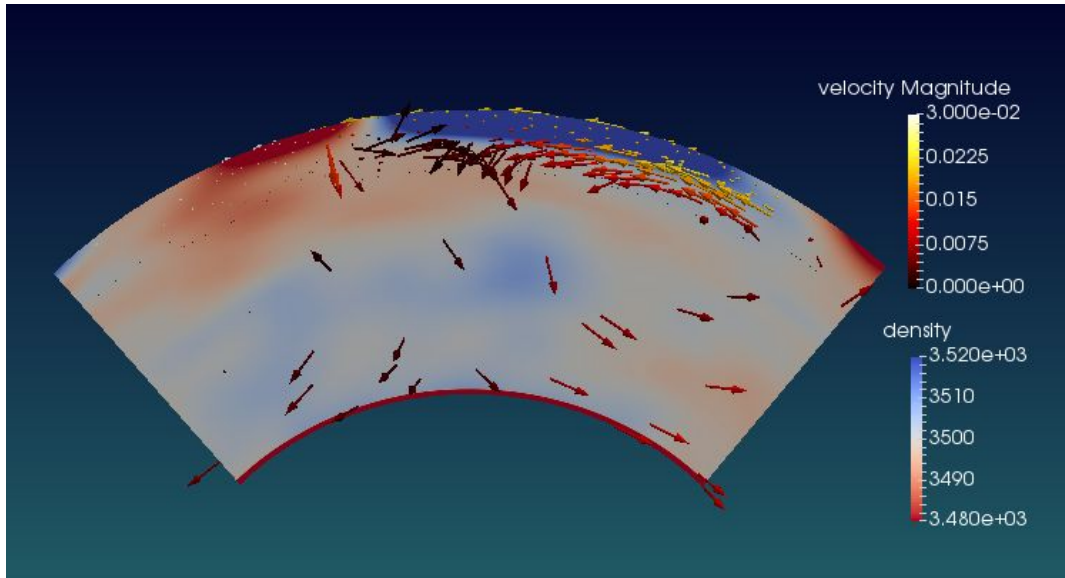
which the particles on the inner boundary $r = 1$ have traveled one revolution. It is apparent from the image on the right that with the arithmetic averaging interpolant, the particles cease to cover all of the finite element cells leaving gaps in the distribution of the particles, whereas in the image on the left the distribution of particles is over the entire domain and, in particular, each cell has at least the three particles that are required to determine the bilinear interpolant with the least squares method.

Regionally high resolution 3D spherical flow model with weak plate boundaries

Wanying Wang

Compared to the interior of the plates, plate boundaries are weaker. Here I present a 3D spherical mantle flow model with the viscosity at the plate boundaries assigned to be weaker than regular lithosphere. The density structure is assigned by reading in SMEAN tomography model. The model is regionally refined to reach the resolution of ~ 15 km/cell.

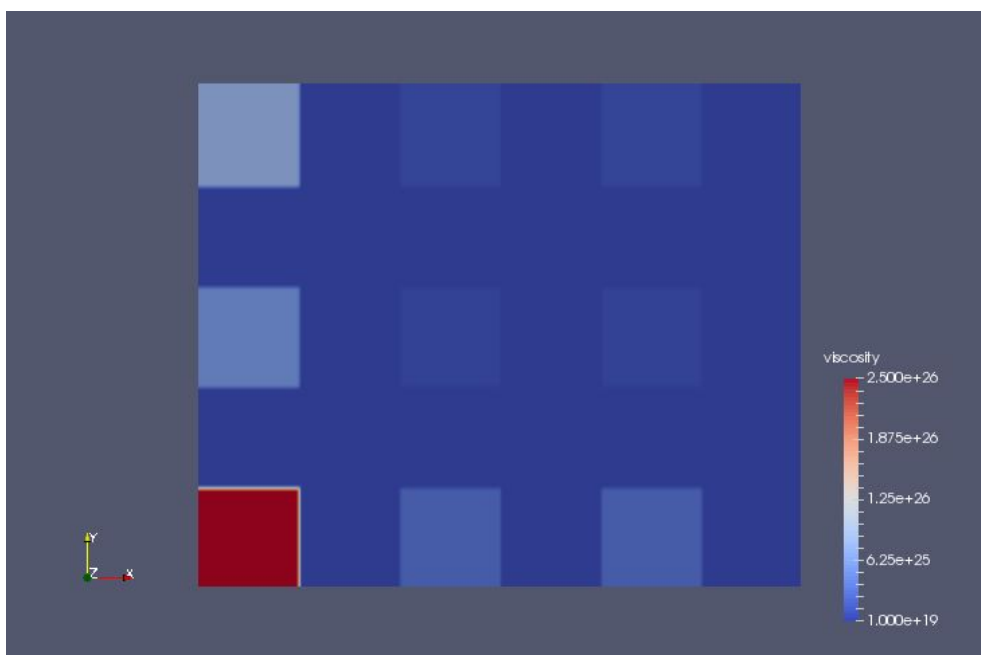




Implement lateral viscosity variations for multiple structures

Wanying Wang

The viscosity structure shown in the plot below is resulted from a 5-layer radial viscosity variation combines the Lateral Viscosity Variations. The LVVs are assigned using 6 compositions that each has a different viscosity prefactor, and they forms 6 vertical stripes. This approach can be used to assign a multi-component LVVs structure in a 3D spherical mantle flow model.



Statistics about ASPECT's growth during the hackathon

The following contains a number of statistics about how much ASPECT has grown during the hackathon:

- Number of source files in ASPECT before/after: 497 -> 509 +12
- Lines of code in ASPECT before/after: 120,058 -> 124,162 +4,104
- Number of merged pull requests before/after: 1595 -> 1771 +176
- Commits in github before/after: 5705 -> 6012 +307
- Number of tests before/after: 583 -> 608 +25

These numbers are a significant increase over the previous hackathon. (The added number of source lines of code is depressed by the merge of a number of patches that reduce the size of ASPECT significantly by replacing code blocks that have been repeated throughout the code base many times, by a single function call that refactors this code.) For comparison, these were the statistics for last year's (2017) hackathon:

- Number of source files in ASPECT before/after: 449 -> 466 +17
- Lines of code in ASPECT before/after: 97,055 -> 102,826 +5,771
- Number of merged pull requests before/after: 1023 -> 1210 +187
- Commits in github before/after: 4,545 -> 4,893 +338
- Number of tests before/after: 436 -> 476 +40

The difference between the second number here (at the end of the 2017 hackathon) and the first number in each column of the table above it (at the start of the 2018 hackathon) illustrates the level of development that happened over the course of the year between the hackathons.

These statistics were generated through the following commands:

- `find include/ source/ | egrep '\.(h|cc)$' | wc -l`
- `cat `find include/ source/ | egrep '\.(h|cc)$'` | wc -l`
- `git log --format=oneline | grep "Merge pull request" | wc -l`
- `git log --format=oneline | grep -v "Merge pull request" | wc -l`
- `ls -l tests/*prm | wc -l`

References

- Holland, T. J. and Powell, R. (2011), An improved and extended internally consistent thermodynamic dataset for phases of petrological interest, involving a new equation of state for solids. *Journal of Metamorphic Geology*, 29: 333-383.
[doi:10.1111/j.1525-1314.2010.00923.x](https://doi.org/10.1111/j.1525-1314.2010.00923.x)
- Tosi, N, et al. (2015) "A community benchmark for viscoplastic thermal convection in a 2-D square box." *Geochemistry, Geophysics, Geosystems* 16.7: 2175-2196.
- Biryol, C. B., Wagner, L. S., Fischer, K. M., & Hawman, R. B. (2016). Relationship between observed upper mantle structures and recent tectonic activity across the southeastern United States. *Journal of Geophysical Research: Solid Earth*, 121(5), 3393-3414.
- Schaeffer, A. J., & Lebedev, S. (2013). Global shear speed structure of the upper mantle and transition zone. *Geophysical Journal International*, 194(1), 417-449.
- Rudi, J., Stadler, G., & Ghattas, O. (2017). Weighted BFBT Preconditioner for Stokes Flow Problems with Highly Heterogeneous Viscosity. *SIAM Journal on Scientific Computing*, 39(5), S272-S297.
- May, D. A., Brown, J., & Le Pourhet, L. (2015). A scalable, matrix-free multigrid preconditioner for finite element discretizations of heterogeneous Stokes flow. *Computer methods in applied mechanics and engineering*, 290, 496-523.
- Matthews, K. J., Maloney, K. T., Zahirovic, S., Williams, S. E., Seton, M., & Mueller, R. D. (2016). Global plate boundary evolution and kinematics since the late Paleozoic. *Global and Planetary Change*, 146, 226-250.
- Kaus, B. J. (2010). Factors that control the angle of shear bands in geodynamic numerical models of brittle deformation. *Tectonophysics*, 484(1-4), 36-47.
- Donea, J., & Huerta, A. (2003). *Finite element methods for flow problems*. John Wiley & Sons.
- Dunn, R. A., & Forsyth, D. W. (2003). Imaging the transition between the region of mantle melt generation and the crustal magma chamber beneath the southern East Pacific Rise with short-period Love waves. *Journal of Geophysical Research: Solid Earth*, 108(B7).
- Kaminski, É., & Ribe, N. M. (2002). Timescales for the evolution of seismic anisotropy in mantle flow. *Geochemistry, Geophysics, Geosystems*, 3(8), 1-17.
- Arrial, P. A., Flyer, N., Wright, G. B., & Kellogg, L. H. (2014). On the sensitivity of 3-D thermal convection codes to numerical discretization: a model intercomparison.